

University of Nebraska - Lincoln

DigitalCommons@University of Nebraska - Lincoln

USGS Staff -- Published Research

US Geological Survey

2013

Using hand proportions to test taxonomic boundaries within the *Tupaia glis* species complex (Scandentia, Tupaiidae)

Eric J. Sargis

Yale University, eric.sargis@yale.edu

Neal Woodman

U.S. Geological Survey

Aspen T. Reese

Yale University

Link E. Olson

University of Alaska Fairbanks

Follow this and additional works at: <https://digitalcommons.unl.edu/usgsstaffpub>

Sargis, Eric J.; Woodman, Neal; Reese, Aspen T.; and Olson, Link E., "Using hand proportions to test taxonomic boundaries within the *Tupaia glis* species complex (Scandentia, Tupaiidae)" (2013). *USGS Staff -- Published Research*. 717.

<https://digitalcommons.unl.edu/usgsstaffpub/717>

This Article is brought to you for free and open access by the US Geological Survey at DigitalCommons@University of Nebraska - Lincoln. It has been accepted for inclusion in USGS Staff -- Published Research by an authorized administrator of DigitalCommons@University of Nebraska - Lincoln.

Using hand proportions to test taxonomic boundaries within the *Tupaia glis* species complex (Scandentia, Tupaiidae)

ERIC J. SARGIS,* NEAL WOODMAN, ASPEN T. REESE, AND LINK E. OLSON

Department of Anthropology, Yale University, P.O. Box 208277, New Haven, CT 06520, USA (EJS)

Department of Ecology and Evolutionary Biology, Yale University, P.O. Box 208106, New Haven, CT 06520, USA (EJS, ATR)

Division of Vertebrate Zoology, Yale Peabody Museum of Natural History, New Haven, CT 06520, USA (EJS, ATR)

United States Geological Survey, Patuxent Wildlife Research Center, National Museum of Natural History, Smithsonian Institution, Washington, DC 20013, USA (NW)

University of Alaska Museum, University of Alaska Fairbanks, Fairbanks, AK 99775, USA (LEO)

* Correspondent: eric.sargis@yale.edu

Treeshrews (order Scandentia) comprise 2 families of squirrel-sized terrestrial, arboreal, and scansorial mammals distributed throughout much of tropical South and Southeast Asia. The last comprehensive taxonomic revision of treeshrews was published in 1913, and a well-supported phylogeny clarifying relationships among all currently recognized extant species within the order has only recently been published. Within the family Tupaiidae, 2 widely distributed species, the northern treeshrew, *Tupaia belangeri* (Wagner, 1841), and the common treeshrew, *T. glis* (Diard, 1820), represent a particularly vexing taxonomic complex. These 2 species are currently distinguished primarily based on their respective distributions north and south of the Isthmus of Kra on the Malay Peninsula and on their different mammae counts. This problematic species complex includes 54 published synonyms, many of which represent putative island endemics. The widespread *T. glis* and *T. belangeri* collectively comprise a monophyletic assemblage representing the sister lineage to a clade composed of the golden-bellied treeshrew, *T. chrysogaster* Miller, 1903 (Mentawai Islands), and the long-footed treeshrew, *T. longipes* (Thomas, 1893) (Borneo). As part of a morphological investigation of the *T. glis*–*T. belangeri* complex, we studied the proportions of hand bones, which have previously been shown to be useful in discriminating species of soricids (true shrews). We measured 38 variables from digital X-ray images of 148 museum study skins representing several subspecies of *T. glis*, *T. belangeri*, *T. chrysogaster*, and *T. longipes* and analyzed these data using principal components and cluster analyses. Manus proportions among these 4 species readily distinguish them, particularly in the cases of *T. chrysogaster* and *T. longipes*. We then tested the distinctiveness of several of the populations comprising *T. glis* and *T. longipes*. *T. longipes longipes* and *T. l. salatana* Lyon, 1913, are distinguishable from each other, and populations of *T. “glis”* from Bangka Island and Sumatra are distinct from those on the Malay Peninsula, supporting the recognition of *T. salatana*, *T. discolor* Lyon, 1906, and *T. ferruginea* Raffles, 1821 as distinct species in Indonesia. These relatively small, potentially vulnerable treeshrew populations occur in the Sundaland biodiversity hotspot and will require additional study to determine their appropriate conservation status.

Key words: digits, manus, morphology, postcranium, rays, skeleton, Southeast Asia, treeshrews

© 2013 American Society of Mammalogists

DOI: 10.1644/11-MAMM-A-343.1

Treeshrews (order Scandentia) are small-bodied mammals found throughout much of South and Southeast Asia, including many islands of the Sunda Shelf. Although superficially resembling squirrels, treeshrews were included in the order Primates for much of the last century (e.g., Carlsson 1922; Napier and Napier 1967). When they were removed from Primates, they were placed in their own order, Scandentia

(Butler 1972), and are typically included in the supraordinal grouping Euarchonta with Dermoptera (colugos) and Primates (e.g., Bloch et al. 2007; Janecka et al. 2007; Murphy et al.



2001). Relationships within Euarchonta remain controversial, and treeshrews have been considered alternatively the sister taxon of Dermoptera (Sundatheria—Bloch et al. 2007; Murphy et al. 2001), Primates (Liu et al. 2009), and a Primates–Dermoptera clade (Primates—Janecka et al. 2007). Most recently, they were supported as the sister of a Rodentia–Lagomorpha clade (Glires—Meredith et al. 2011).

Despite the broad interest in the interordinal relationships of treeshrews stimulated by their potentially close relationship with Primates, intraordinal relationships had been largely ignored until recently. Early molecular investigations of treeshrew interrelationships were phenetic studies based on either immunodiffusion distances (Dene et al. 1978, 1980) or DNA–DNA hybridization (Han et al. 2000) and, therefore, not readily amenable to testing alternative hypotheses or assessing support for groupings. Furthermore, taxon sampling was extremely limited in these studies, with inclusion of only 6 (Han et al. 2000) to 9 (Dene et al. 1978, 1980) of the 20 currently recognized species (Helgen 2005).

More-recent studies provide an intraordinal phylogenetic framework in which evolutionary and biogeographic patterns can be explored in greater detail. Olson et al. (2004b) reanalyzed published morphological data in parsimony analyses, and Olson et al. (2005) conducted the 1st analysis of treeshrew interrelationships based on DNA sequence data, analyzing the mitochondrial 12S rRNA gene from 16 species representing all 5 currently recognized genera. Roberts et al. (2009) conducted a phylogenetic analysis of 6 nuclear genes in 11 species and followed up with a phylogenetic analysis and divergence date estimates based on the contiguous mitochondrial ribosomal genes 12S, tRNA-Val, and 16S from each of the 20 recognized species (Roberts et al. 2011).

These recent phylogenetic analyses of interspecific relationships among treeshrews have implications for the taxonomy of the group, which has a tortuous history and has not been comprehensively studied since Lyon's (1913) monographic revision a century ago, in which he recognized 46 species (and 35 additional subspecies) of treeshrews. Leading up to and following Lyon's (1913) taxonomic treatment of the group, there was a proliferation of species and subspecies descriptions through the 1st half of the 20th century, with a subsequent era of synonymization resulting in a dramatic decrease in the number of recognized species (see Fig. 1). In recent years, this number has varied from 16 (Corbet and Hill 1980, 1992; Honacki et al. 1982) to 19 (Duff and Lawson 2004; Wilson 1993) or 20 (Helgen 2005) species. Species boundaries are particularly poorly defined in *Tupaia*, a genus that Wilson (1993:131) characterized as being “badly in need of review.” Among *Tupaia*, the most problematic taxa have been the 54 named forms now synonymized with *T. glis* (Diard, 1820), the common treeshrew, and *T. belangeri* (Wagner, 1841), the northern treeshrew (Helgen 2005). Within this complex, various authorities have recognized as many as 10 species (Lyon 1913) or as few as 1 (Napier and Napier 1967). Adding to this confusion, decisions regarding synonymy have often been inconsistent among taxonomists (see below).

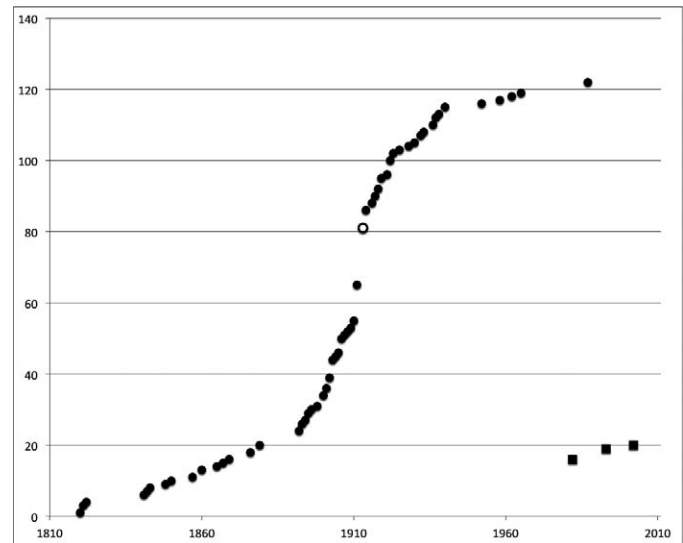


FIG. 1.—Accumulation curve of the total number of described species and subspecies (circles) of treeshrews from 1820, when the 1st species was described, to present. Squares represent the number of species recognized in the 3 editions of *Mammal Species of the World* (Helgen 2005; Honacki et al. 1982; Wilson 1993). Open circle indicates the last formal revision of Scandentia by Lyon (1913).

Criteria used to delineate species and subspecies of *Tupaia* have been dominated by external characters, primarily subtle differences in pelage color (Steele 1983). Hill (1960), however, demonstrated that among mainland populations identified as *T. glis* and *T. belangeri*, much of this pelage variation is continuously distributed along a latitudinal cline, with no clear discontinuities separating the 2 species. A similar cline is evident among populations on islands adjacent to the Malay Peninsula (Hill 1960). Napier and Napier (1967) subsequently referred all of these populations to *T. glis*. In contrast, Martin (1968) recognized all mainland forms of *Tupaia* north of the Isthmus of Kra ($\sim 10^\circ$ N latitude), most of which possess 6 mammae, as *T. belangeri*, and those distributed south of the isthmus, which have only 4 mammae, as *T. glis* (Table 1). The separation of *T. belangeri* and *T. glis* was supported by Olson et al. (2005), but more recent molecular studies employing additional data and taxa suggest that the 2 are not reciprocally monophyletic, at least over the coalescent history of their mitochondrial genomes (Roberts et al. 2009; Roberts et al. 2011). Maximum divergence in the 12S gene between individual specimens identified as *T. glis* and *T. belangeri* (Olson et al. 2005) can exceed that between *Homo* and *Pan* and even that between *Mus* and *Rattus* (Olson and Yoder 2002). *T. glis* and *T. belangeri* also have been distinguished in a bioacoustical analysis of their loud (chatter) calls (Esser et al. 2008).

Although the distinction between *T. glis* and *T. belangeri* has been accepted by most recent authors (e.g., Helgen 2005), affiliation of individual taxa described from the region surrounding the Isthmus of Kra has been inconsistent. *Tupaia lacernata kohtauensis* Shamel, 1930, *T. ferruginea operosa* Robinson and Kloss, 1914, and *T. f. ultima* Robinson and

TABLE 1.—Distribution of discrete features of *Tupaia* discussed in the text.

Taxon	Distribution	No. mammae	Presence of entepicondylar foramen
<i>T. glis</i>	Southern Malay Peninsula	4	Present ^a
<i>T. ferruginea</i>	Sumatra	4	Present ^b
<i>T. g. hypochrysa</i>	Java	4	Absent ^c
<i>T. discolor</i>	Bangka Island	6	Absent ^d
<i>T. belangeri</i>	North of Isthmus of Kra	6	Present ^e
<i>T. longipes</i>	Northern Borneo	6	Absent ^f
<i>T. salataana</i>	Southern Borneo	6	Absent ^g
<i>T. chrysogaster</i>	Mentawai Islands	2	Absent ^h

^a Field Museum of Natural History (FMNH; Chicago, Illinois) 98468–98470.^b Museum of Comparative Zoology (MCZ; Cambridge, Massachusetts) 6276; Naturhistorisches Museum Basel (Basel, Switzerland) 2992.^c Rijksmuseum van Natuurlijke Historie (Leiden, Netherlands) 36116.^d United States National Museum (USNM; Smithsonian Institution, Washington, D.C.) 124698.^e American Museum of Natural History (AMNH; New York, New York) 113135; MCZ 35810, 35812–35819, 35821, 35823–35825, 35827, 35830, 35839–35842; Museum of Vertebrate Zoology (Berkeley, California) 68783, 119721; Muséum National d'Histoire Naturelle (MNHN; Paris, France) 1970-175, 1990-501–1990-506, 1990-508–1990-512; USNM 583793–583795, 583817, 584375, 584376; Yale Peabody Museum of Natural History (New Haven, Connecticut) 310, 311.^f FMNH 76815, 76819, 76824, 76825; MCZ 35614; MNHN 1977-362; USNM 396664–396667, 396673.^g Royal Ontario Museum (Toronto, Ontario, Canada) 101993; USNM 198043, 199162.^h USNM 121883 (X-ray).

Kloss, 1914, for example, were referred to *T. glis* by Corbet and Hill (1992), but were later reallocated without explanation to *T. belangeri* (Helgen 2005; Wilson 1993). Analysis of pelage color and craniodontal measurements among purported *T. glis* from the Hat-Yai region of southern peninsular Thailand revealed the sympatric occurrence of 2 discrete morphotypes (Endo et al. 2000b), an observation interpreted as range overlap between *T. glis* and *T. belangeri* 3° south of the previously recognized contact zone (Endo et al. 2000b; Helgen 2005). Co-occurrence of the 2 putative species has since been confirmed in a cytogenetic study (Hirai et al. 2002). The fact that Lyon (1913) recorded individuals north of the Isthmus of Kra with only 2 pairs of mammae suggests that the contact zone may be broader than suspected.

Some taxa once considered synonymous with *T. glis* can be distinguished by mammae formula. The long-footed treeshrew, *Tupaia longipes* (Thomas, 1893), from Borneo, has 6 mammae, whereas the golden-bellied treeshrew, *T. chrysogaster* Miller, 1903, endemic to the Mentawai Islands off the west coast of Sumatra, is characterized by the presence of only 2 mammae. The separation of *T. longipes* and *T. chrysogaster* from *T. glis* also is supported by molecular analyses (Olson et al. 2005; Roberts et al. 2009; Roberts et al. 2011). A population from Bangka Island off the east coast of Sumatra that was recognized as a distinct species (*T. discolor* Lyon, 1906) by Lyon (1913), but currently referred to *T. glis* (Helgen 2005), possesses the 6 mammae typical of *T. belangeri* and *T. longipes*, whereas other taxa currently synonymized with *T. glis*, such as *T. “glis” ferruginea* (Raffles, 1821) from Sumatra

and *T. “glis” hypochrysa* (Thomas, 1895) from Java, have the 4 mammae typical of *T. glis* (Table 1).

Morphometric features have occasionally featured in the recognition of taxonomic boundaries among species of *Tupaia*. For example, Thomas' (1917) description of *T. clarissa* (now referred to *T. belangeri*) from southern peninsular Myanmar was based on differences in skull size relative to more northerly populations. Thomas (1917:199) further remarked on the “complete absence of intermediate specimens” in this region. Until very recently, geographic variation in body size within treeshrew species received little, if any, attention. Based on cranial measurements, Endo et al. (2000a) showed that specimens referred to *T. glis* from south of the Isthmus of Kra were morphometrically distinct from specimens identified as *T. belangeri* collected north of the Isthmus (from Thailand and Laos), although no clear patterns were identified.

In our morphological evaluation of the *T. glis* species complex, we examined variation in proportions of the hand (manus) bones. Morphology of the forelimb and manus has long been recognized as diagnostically useful at higher taxonomic levels among mammals (e.g., Carroll 1988; Kardong 1998; Owen 1866; Vaughan 1970) and has more recently been used successfully to differentiate closely related species of soricids (Woodman 2010, 2011; Woodman and Morgan 2005; Woodman and Stephens 2010), which, like treeshrews, are a group rife with cryptic species lacking obvious diagnostic characteristics. Although various aspects of the treeshrew forelimb, including the manus, have been studied (e.g., Sargis 2002a; Stafford and Thorington 1998), the focus of these studies has been on the carpus rather than hand proportions. As with many other mammalian taxa, few cleaned and intact skeletons of the manus of tupaiids are available for study (see Sargis 2002a). Fortunately, traditional methods of preparing dried skins of small mammals for systematic study leave bones of the hands within the dried skins in their relative positions. Following methods described by Woodman and Morgan (2005), we imaged the manus skeleton in dried skins with a digital X-ray system and used the resulting images to quantify intraspecific and interspecific variability among treeshrew taxa.

MATERIALS AND METHODS

We X-rayed the right and left manus of 148 dried study skins of tupaiids using a Kevex–Varian digital X-ray system in the Museum Support Center of the United States National Museum of Natural History (USNM), Suitland, Maryland. Forefeet were X-rayed at 30 kV, 356 µA with a Thermo Scientific Kevex X-ray source interfaced with a desktop computer using Kevex X-ray Source Control Interface (version 4.1.3; Palo Alto, California). Digital images were constructed using Varian Medical Systems Image Viewing and Acquisition (VIVA version 2.0; Waltham, Massachusetts) and then transferred to Adobe Photoshop CS4 Extended (version 11.0.2; Adobe Systems Inc., San Jose, California), trimmed, and converted to positive images (Fig. 2). One of us (ATR)

quantified variation in the metacarpals and phalanges of the manus by measuring the images of these elements with the custom Measurement Scale in the Analysis menu of Adobe Photoshop. A list of the taxa we investigated for this study, and the specimens we assigned to each, is provided in Appendix I.

Measurements were taken from the most complete image of either the right or left side, and supplemented, where necessary and possible, by measurements from the image of the other side. We recorded the following measurements from all 5 rays (38 total), with the exception that depths (dorsopalmar distances) of bones were substituted for widths (mediolateral distances) in ray I because of its orientation in the images: DPD = distal phalanx depth; DPL = distal phalanx length; DPW = distal phalanx width; MD = metacarpal depth; ML = metacarpal length; MW = metacarpal width; MPL = middle phalanx length; MPW = middle phalanx width; PPD = proximal phalanx depth; PPL = proximal phalanx length; PPW = proximal phalanx width (Fig. 2). All measurements are in millimeters and are rounded to the nearest 0.01 mm. Tabled summary statistics include mean, standard deviation, and total range (Table 2).

We conducted principal components analysis (PCA) individually on each ray, and occasionally by combining data from different rays, to investigate variation in digit proportions among taxa at each stage of our study. In general, however, we avoided combining variables from different rays because the resulting models were too parameter-rich to interpret. Because the results of our analyses provided evidence for the possible recognition of additional taxa, our investigation was conducted in 6 stages represented by different numbers of taxa and different compositions of certain taxa. Our initial analyses involved 4 previously recognized species (Helgen 2005)—*T. belangeri*, *T. chrysogaster*, *T. glis*, and *T. longipes*—and ultimately included 8 taxa that we eventually interpreted as being taxonomically distinct (Appendix I): *T. belangeri*, *T. chrysogaster*, *T. “glis” discolor* (Bangka Island), *T. “glis” ferruginea* (i.e., all *T. glis* from Sumatra), *T. “glis” hypochrysa* (Java), *T. glis* (all subspecies, but see caveat below), *T. longipes longipes*, and *T. longipes salatana* Lyon, 1913. Because 3 taxa (*T. “glis” discolor*, *T. “glis” ferruginea*, and *T. “glis” hypochrysa*) were sequentially removed from *T. glis* during the course of our study, the composition of *T. glis* varied. Similarly, *T. longipes* was eventually split into *T. l. longipes* and *T. l. salatana*.

In all cases except our initial test of the 4 currently recognized species, we analyzed taxon mean values and variation among individuals. The advantage of analyzing means is that the procedure permits us to utilize variables that are missing from individual specimens, which would exclude these specimens from the analyses and reduce the effective sample size considerably. Because of the resulting completeness of the data set, the most useful variables can be selected for a particular analysis. To compare some synonymized taxa more closely with *T. glis*, we also analyzed individuals. This type of analysis permits us to assess variance within and between groups, determine how much overlap in morpholog-

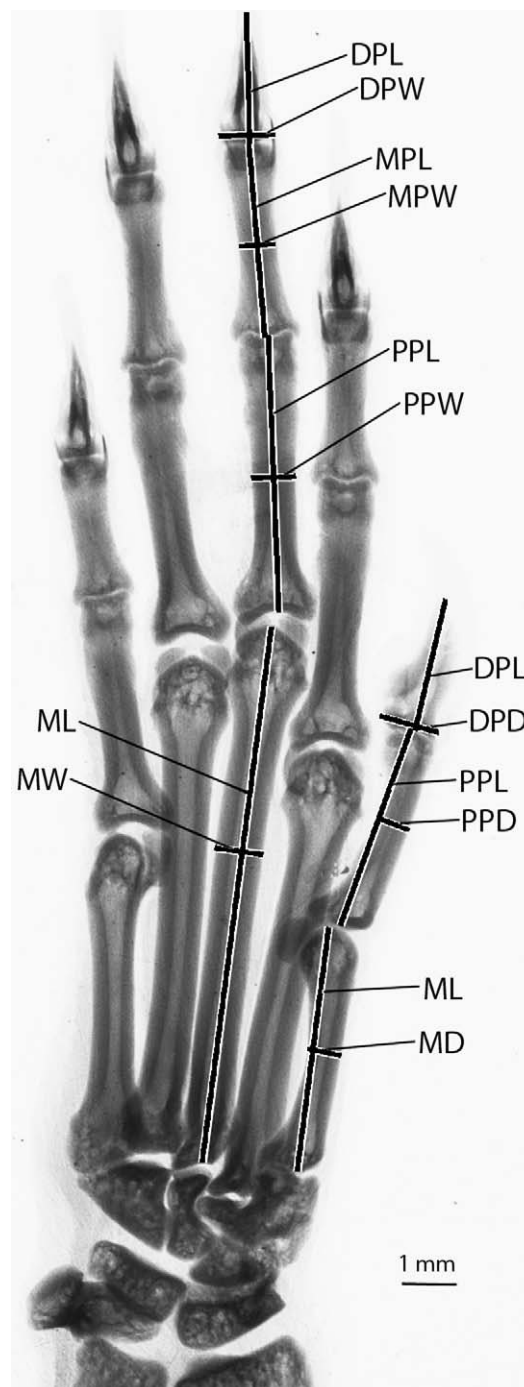


FIG. 2.—Digital X-ray of the right manus (plantar view) of *Tupaia belangeri* (USNM 201431), illustrating the measurements used in this study. DPD = distal phalanx depth; DPL = distal phalanx length; DPW = distal phalanx width; MD = metacarpal depth; ML = metacarpal length; MW = metacarpal width; MPL = middle phalanx length; MPW = middle phalanx width; PPD = proximal phalanx depth; PPL = proximal phalanx length; PPW = proximal phalanx width. Original negative was converted to a positive image.

ical space exists between taxa, and examine outliers. Because of missing data, analyses involving individuals are generally a compromise between number of variables and number of specimens. For this reason, the models used for analyses of

means versus individuals utilize different variables and result in different patterns in morphospace.

In addition to PCA, we performed hierarchical cluster analyses on the 38 variables from all 5 rays to determine the similarity of hand proportions among taxa. Phenograms from these analyses are presented with Euclidean distances.

Four taxa.—Our initial objective in studying the hands of *Tupaia* was to determine whether characteristics of the skeleton of the manus would help to distinguish the closely related species *T. belangeri*, *T. chrysogaster*, *T. glis*, and *T. longipes*. The 4 taxa in this 1st analysis were *T. belangeri*, *T. chrysogaster*, *T. glis* (*T. glis* + *T. “glis” ferruginea* + *T. “glis” discolor* + *T. “glis” hypochrysa*), and *T. longipes* (*T. l. longipes* + *T. l. salatana*).

Five taxa.—In the 2nd stage of our investigation, we examined the distinctiveness of the Bangka Island population, *T. “glis” discolor*, by contrasting it with the 4 currently recognized species. This stage included 5 groups: *T. belangeri*, *T. chrysogaster*, *T. glis* (*T. glis* + *T. “glis” ferruginea* + *T. “glis” hypochrysa*), *T. “glis” discolor*, and *T. longipes* (*T. l. longipes* + *T. l. salatana*).

Subspecies of *Tupaia longipes*.—The 3rd stage examined differentiation of 2 subspecies of *T. longipes* (*T. l. longipes* and *T. l. salatana*) that occur in distinct regions of Borneo. In our search for potential differences between these 2 taxa, we again carried out PCA on each of the 5 rays individually. Because of the small sample sizes, we used only variables with complete data for all specimens (except for ray V, for which complete data were available for only 6 specimens). This restriction resulted in only 3 or 4 variables being available for each ray. To construct a more comprehensive data set, we also performed a PCA on 10 variables combined from rays I, IV, and V because those rays had the most distinctive variables.

Six taxa.—In the 4th stage of our investigation, we attempted to determine both how well *T. l. longipes* and *T. l. salatana* were differentiated when compared with the other 4 taxa (*T. belangeri*, *T. chrysogaster*, *T. glis* [*T. glis* + *T. “glis” ferruginea* + *T. “glis” hypochrysa*], and *T. “glis” discolor*), and, consequently, how treatment of *T. l. longipes* and *T. l. salatana* as separate taxa affected the distinctiveness of those other taxa.

Seven taxa.—The 5th stage examined the distinctiveness of all *T. glis* from the island of Sumatra (referred to herein as *T. “glis” ferruginea*) from all other *T. glis*, resulting in 7 taxon groups: *T. glis* (*T. glis* + *T. “glis” hypochrysa*), *T. “glis” ferruginea*, *T. “glis” discolor*, *T. belangeri*, *T. chrysogaster*, *T. l. longipes*, and *T. l. salatana*. This stage also examined the effect the removal of Sumatran forms had on the distinctiveness of *T. glis* and *T. “glis” discolor*.

Javan *Tupaia “glis” hypochrysa*.—Our ability to separate Sumatran *T. “glis” ferruginea* from other *T. glis* in the previous stage led us to examine Javan *T. “glis”* (i.e., *T. “glis” hypochrysa*) as well. We had only a single specimen of *T. “glis” hypochrysa* available to us, so we limited our study to PCA and cluster analyses of *T. glis* and 3 island forms: *T. chrysogaster*, *T. “glis” ferruginea*, and *T. “glis” hypochrysa*.

T. chrysogaster was included here because Lyon (1913) paired this taxon with *T. hypochrysa* in his “*Hypochrysa* Group.”

Much of the variation in the proportions of the bones of the manus at higher taxonomic levels can be clearly associated with ecological and behavioral characteristics (e.g., Kirk et al. 2008; Weisbecker and Schmid 2007), as well as phylogeny (e.g., Owen 1866). However, the forefeet of the closely related *Tupaia* taxa we studied tend to be quite conservative, with proportional variation typically measured in fractions of millimeters. These taxa are similar in body size, substrate preference, and general locomotor behavior (e.g., Emmons 2000; Kawamichi and Kawamichi 1979; Langham 1982), and the subtle variation we documented is unlikely to be substantial enough to represent adaptive features related to locomotion. It more likely represents smaller-scale variation within a broader adaptive constraint at a higher taxonomic level. The lack of major functional differences in other aspects of the postcrania of these *Tupaia* taxa (Sargis 2001, 2002a, 2002b) supports this view.

RESULTS

Four taxa.—Although our investigation of the hand proportions of *T. glis*, *T. belangeri*, *T. chrysogaster*, and *T. longipes* included PCA of each individual ray, our discussion focuses on ray IV because this analysis yielded the greatest separation among the 4 species. A bivariate plot of the first 2 factors from the PCA of ray IV is shown in Fig. 3A. Factor 1, which accounts for nearly 75% of the total variance (Table 3), represents size, and factor 2, representing almost 20% of the total variance, is a shape factor most highly influenced in this analysis by the negatively weighted variables DPL and DPW (Table 3). For ray IV proportions, *T. glis* and *T. belangeri* are nearly the same size, and both are much smaller than either *T. chrysogaster* or *T. longipes*, especially the latter. Along the 2nd factor axis, *T. glis* and *T. longipes* exhibit short, narrow distal phalanges, although these characteristics are more extreme in the latter species. In contrast, *T. chrysogaster* has relatively long, wide distal phalanges, and *T. belangeri* is more nearly average in its proportions.

Similar plots of PCA scores from the other 4 rays (not shown) exhibit the same general size relationships, indicating that the rays of *T. glis* and *T. belangeri* are small relative to those of *T. chrysogaster* and *T. longipes*. The 2nd factor axis in each of these analyses also is dominated by DPL and DPW, except in that for ray V, in which the variables with the greatest influence are MPW and DPL. The 2nd factor scores from each of these analyses indicate that *T. glis* and *T. belangeri* are generally closest to average proportions of the distal phalanx for these 4 species, whereas *T. chrysogaster* has the largest and *T. longipes* the smallest distal phalanges.

Cluster analysis of all 38 variables shows that *T. glis* and *T. belangeri* are most similar to each other, with *T. chrysogaster* as the next most similar species (Fig. 3B). *T. longipes* is the least similar to the other 3 species.

TABLE 2.—Measurements of bones (in mm) in the manus of selected taxa of *Tupaia*. Variations in sample size appear in parentheses. Because of its orientation in the X-rays, depth was measured for ray I; width was measured for the other 4 rays (see “Materials and Methods”).

	Metacarpal length (ML)	Metacarpal depth/width (MD/MW)	Proximal phalanx length (PPL)	Proximal phalanx depth/width (PPD/PPW)	Middle phalanx length (MPL)	Middle phalanx width (MPW)	Distal phalanx length (DPL)	Distal phalanx depth/width (DPD/DPW)
Ray I								
<i>T. belangeri</i>	4.18 ± 0.30 3.60–4.92 (71)	0.59 ± 0.06 0.47–0.79 (66)	3.37 ± 0.23 2.56–3.92 (72)	0.61 ± 0.06 0.43–0.79 (71)	—	—	2.41 ± 0.18 1.88–2.89 (66)	1.00 ± 0.10 0.81–1.23 (55)
<i>T. chrysogaster</i>	4.53 ± 0.25 4.09–4.88 (12)	0.70 ± 0.05 0.61–0.79 (12)	3.45 ± 0.32 2.77–3.93 (12)	0.69 ± 0.06 0.61–0.80 (12)	—	—	2.57 ± 0.17 2.25–2.82 (11)	1.24 ± 0.13 1.07–1.45 (12)
<i>T. glis</i>	4.20 ± 0.28 3.59–5.13 (32)	0.59 ± 0.07 0.49–0.84 (32)	3.34 ± 0.17 2.90–3.76 (31)	0.62 ± 0.07 0.50–0.79 (31)	—	—	2.36 ± 0.27 1.47–2.94 (31)	1.04 ± 0.12 0.87–1.27 (28)
<i>T. g. discolor</i>	4.99 ± 0.23 4.71–5.25 (6)	0.62 ± 0.04 0.55–0.66 (6)	3.18 ± 0.08 3.11–3.30 (6)	0.62 ± 0.03 0.58–0.66 (6)	—	—	2.27 ± 0.17 2.05–2.47 (5)	1.26 ± 0.05 1.20–1.33 (5)
<i>T. g. ferruginea</i>	4.57 ± 0.28 3.91–4.96 (14)	0.62 ± 0.05 0.52–0.72 (14)	3.54 ± 0.18 3.11–3.74 (14)	0.64 ± 0.05 0.57–0.72 (14)	—	—	2.44 ± 0.19 1.98–2.73 (13)	1.19 ± 0.16 0.96–1.41 (13)
<i>T. g. hypochrysa</i>	4.40	0.64	3.64	0.60	—	—	2.78	1.08
<i>T. longipes longipes</i>	4.87 ± 0.19 4.66–5.02 (3)	0.76 ± 0.04 0.73–0.80 (3)	3.52 ± 0.09 3.44–3.61 (3)	0.72 ± 0.03 0.69–0.75 (3)	—	—	2.56 ± 0.12 2.43–2.65 (3)	1.11 ± 0.18 0.94–1.29 (3)
<i>T. l. salatana</i>	5.10 ± 0.09 4.97–5.16 (4)	0.67 ± 0.02 0.64–0.68 (4)	3.58 ± 0.04 3.53–3.63 (4)	0.68 ± 0.03 0.64–0.71 (4)	—	—	2.41 2.38–2.44 (2)	1.13 ± 0.02 1.11–1.15 (3)
Ray II								
<i>T. belangeri</i>	7.76 ± 0.65 6.80–9.50 (61)	0.75 ± 0.07 0.60–0.95 (59)	4.45 ± 0.28 3.85–5.19 (71)	0.73 ± 0.07 0.62–0.89 (56)	2.71 ± 0.25 2.16–3.23 (53)	0.69 ± 0.08 0.54–0.80 (25)	2.33 ± 0.27 1.76–2.98 (60)	1.02 ± 0.06 0.93–1.12 (27)
<i>T. chrysogaster</i>	8.34 ± 0.61 7.33–9.39 (10)	0.83 ± 0.08 0.66–0.91 (8)	4.89 ± 0.22 4.61–5.35 (11)	0.76 ± 0.05 0.67–0.85 (8)	2.82 ± 0.15 2.61–3.01 (9)	0.79 ± 0.04 0.75–0.86 (5)	2.62 ± 0.34 1.85–3.16 (12)	1.11 ± 0.05 1.06–1.18 (7)
<i>T. glis</i>	7.52 ± 0.42 6.91–8.92 (30)	0.72 ± 0.05 0.63–0.84 (27)	4.58 ± 0.31 3.64–5.01 (33)	0.69 ± 0.05 0.57–0.78 (25)	2.76 ± 0.19 2.32–3.20 (28)	0.69 ± 0.07 0.56–0.82 (17)	2.22 ± 0.31 1.65–2.91 (31)	1.02 ± 0.09 0.87–1.23 (14)
<i>T. g. discolor</i>	9.16 ± 0.22 8.89–9.42 (5)	0.75 ± 0.06 0.71–0.83 (4)	4.84 ± 0.10 4.76–5.00 (6)	0.70 ± 0.04 0.65–0.76 (5)	2.85 ± 0.19 2.57–3.12 (6)	0.75 ± 0.04 0.70–0.78 (3)	1.80 ± 0.09 1.73–1.92 (4)	0.96 ± 0.03 0.94–0.98 (2)
<i>T. g. ferruginea</i>	8.10 ± 0.56 6.88–8.95 (14)	0.75 ± 0.05 0.67–0.82 (11)	4.96 ± 0.31 4.35–5.36 (14)	0.71 ± 0.07 0.63–0.89 (12)	2.86 ± 0.20 2.36–3.13 (12)	0.72 ± 0.04 0.67–0.79 (10)	1.98 ± 0.27 1.56–2.39 (12)	1.02 ± 0.06 0.95–1.09 (8)
<i>T. g. hypochrysa</i>	8.46	0.84	5.24	0.71	3.02	0.80	2.34	—
<i>T. l. longipes</i>	9.25 ± 0.14 9.16–9.41 (3)	0.81 ± 0.05 0.78–0.87 (3)	5.19 ± 0.19 4.99–5.36 (3)	0.82 0.78–0.86 (2)	2.76 (1)	0.88 ± 0.12 0.77–1.00 (3)	2.38 ± 0.34 2.07–2.75 (3)	1.00 (1)
<i>T. l. salatana</i>	9.21 ± 0.15 9.08–9.40 (4)	0.82 ± 0.05 0.75–0.85 (4)	5.30 ± 0.11 5.21–5.46 (4)	0.77 ± 0.03 0.74–0.80 (3)	2.78 ± 0.12 2.62–2.90 (4)	0.80 0.80–0.80 (2)	1.94 1.84–2.04 (2)	0.98 0.95–1.01 (2)
Ray III								
<i>T. belangeri</i>	9.54 ± 0.75 8.25–11.73 (63)	0.77 ± 0.06 0.59–0.92 (54)	4.69 ± 0.34 3.84–5.52 (69)	0.78 ± 0.07 0.64–0.98 (64)	3.04 ± 0.40 1.90–3.75 (48)	0.69 ± 0.05 0.57–0.81 (36)	2.36 ± 0.28 1.67–3.00 (64)	0.99 ± 0.08 0.86–1.23 (37)
<i>T. chrysogaster</i>	10.41 ± 0.63 9.55–11.70 (10)	0.82 ± 0.04 0.77–0.89 (10)	5.09 ± 0.17 4.79–5.36 (10)	0.78 ± 0.04 0.71–0.82 (7)	3.06 ± 0.17 2.82–3.37 (10)	0.72 ± 0.03 0.67–0.77 (7)	2.51 ± 0.30 2.27–3.04 (12)	1.12 ± 0.06 1.04–1.18 (5)
<i>T. glis</i>	9.39 ± 0.51 8.60–10.42 (28)	0.75 ± 0.05 0.68–0.86 (24)	4.77 ± 0.29 4.05–5.36 (32)	0.75 ± 0.06 0.65–0.88 (32)	3.01 ± 0.32 2.45–3.76 (28)	0.69 ± 0.06 0.59–0.81 (26)	2.15 ± 0.34 1.61–2.97 (29)	1.05 ± 0.10 0.88–1.23 (17)
<i>T. g. discolor</i>	11.87 ± 0.25 11.53–12.13 (5)	0.82 ± 0.03 0.78–0.86 (5)	5.30 ± 0.31 4.96–5.86 (6)	0.80 ± 0.08 0.69–0.92 (6)	3.00 ± 0.27 2.59–3.32 (6)	0.67 ± 0.05 0.64–0.72 (3)	1.95 ± 0.31 1.63–2.45 (6)	0.96 ± 0.05 0.90–1.03 (4)

TABLE 2.—Continued.

	Metacarpal length (ML)	Metacarpal depth/width (MD/MW)	Proximal phalanx length (PPL)	Proximal phalanx depth/width (PPD/PPW)	Middle phalanx length (MPL)	Middle phalanx width (MPW)	Distal phalanx length (DPL)	Distal phalanx depth/width (DPD/DPW)
<i>T. g. ferruginea</i>	10.25 ± 0.55 9.37–11.20 (13)	0.79 ± 0.05 0.68–0.89 (11)	5.16 ± 0.24 4.73–5.57 (14)	0.73 ± 0.03 0.66–0.78 (14)	3.25 ± 0.24 2.73–3.61 (11)	0.71 ± 0.05 0.66–0.83 (11)	2.06 ± 0.32 1.49–2.45 (12)	1.06 ± 0.07 0.90–1.14 (9)
<i>T. g. hypochrysa</i>	10.96	—	5.56	0.78	3.03	0.79	1.87	—
<i>T. l. longipes</i>	11.48 ± 0.10 11.37–11.55 (3)	0.90 0.85–0.94 (2)	5.49 ± 0.08 5.44–5.59 (3)	0.84 ± 0.03 0.80–0.86 (3)	3.42 (1)	0.77 (2)	2.47 (2)	1.02 (2)
<i>T. l. salatana</i>	11.41 ± 0.14 11.23–11.56 (4)	0.87 ± 0.04 0.83–0.91 (4)	5.63 ± 0.14 5.51–5.80 (4)	0.82 ± 0.05 0.75–0.87 (4)	3.23 3.06–3.39 (2)	0.79 0.74–0.84 (2)	1.96 1.86–2.05 (2)	1.04 (1)
Ray IV								
<i>T. belangeri</i>	8.61 ± 0.63 7.70–10.33 (64)	0.77 ± 0.08 0.57–1.02 (56)	4.57 ± 0.34 3.41–5.32 (68)	0.76 ± 0.06 0.65–0.98 (61)	2.97 ± 0.38 2.04–3.84 (51)	0.70 ± 0.07 0.57–0.88 (38)	2.28 ± 0.32 1.62–2.92 (68)	0.97 ± 0.08 0.73–1.11 (25)
<i>T. chrysogaster</i>	9.51 ± 0.19 9.15–9.81 (8)	0.82 ± 0.06 0.68–0.88 (8)	4.99 ± 0.20 4.70–5.42 (12)	0.78 ± 0.06 0.71–0.89 (9)	3.12 ± 0.19 2.86–3.40 (9)	0.72 ± 0.05 0.66–0.79 (7)	2.60 ± 0.24 2.24–2.95 (12)	1.05 ± 0.10 0.94–1.13 (3)
<i>T. glis</i>	8.56 ± 0.48 7.61–9.57 (28)	0.77 ± 0.07 0.67–0.95 (24)	4.66 ± 0.26 4.09–5.08 (33)	0.72 ± 0.06 0.62–0.83 (31)	2.94 ± 0.34 2.00–3.63 (28)	0.66 ± 0.07 0.56–0.78 (20)	2.22 ± 0.29 1.72–2.89 (28)	0.98 ± 0.09 0.88–1.23 (14)
<i>T. g. discolor</i>	10.31 ± 0.63 9.62–10.85 (3)	0.81 ± 0.07 0.77–0.89 (3)	5.14 ± 0.22 4.85–5.47 (6)	0.69 ± 0.06 0.62–0.79 (6)	2.96 ± 0.27 2.53–3.26 (6)	0.66 ± 0.05 0.60–0.69 (3)	2.00 ± 0.40 1.61–2.55 (4)	—
<i>T. g. ferruginea</i>	9.02 ± 0.55 8.06–9.80 (9)	0.78 ± 0.05 0.71–0.87 (8)	5.04 ± 0.27 4.58–5.47 (14)	0.74 ± 0.05 0.66–0.86 (13)	3.30 ± 0.25 2.85–3.88 (13)	0.71 ± 0.07 0.56–0.82 (11)	2.15 ± 0.32 1.57–2.82 (12)	0.97 ± 0.05 0.90–1.05 (6)
<i>T. g. hypochrysa</i>	9.96	—	5.45	0.82	3.62	0.72	2.60	—
<i>T. l. longipes</i>	10.15 ± 0.34 9.77–10.44 (3)	0.86 ± 0.07 0.78–0.91 (3)	5.36 ± 0.08 5.28–5.43 (3)	0.83 ± 0.03 0.80–0.85 (3)	3.85 (1)	0.77 (2)	2.53 (2)	1.03 (1)
<i>T. l. salatana</i>	10.43 ± 0.23 10.08–10.58 (4)	0.86 ± 0.07 0.77–0.91 (4)	5.40 ± 0.21 5.17–5.63 (4)	0.76 ± 0.06 0.70–0.83 (4)	3.20 ± 0.18 3.09–3.40 (3)	0.73 (1)	2.05 (2)	0.99 (1)
Ray V								
<i>T. belangeri</i>	5.61 ± 0.38 4.87–6.60 (71)	0.76 ± 0.10 0.56–0.99 (63)	3.88 ± 0.27 3.14–4.58 (72)	0.71 ± 0.06 0.60–0.90 (65)	2.29 ± 0.25 1.81–2.97 (40)	0.64 ± 0.08 0.50–0.78 (33)	1.98 ± 0.27 0.72–2.57 (68)	0.93 ± 0.07 0.78–1.05 (37)
<i>T. chrysogaster</i>	5.90 ± 0.33 5.36–6.28 (9)	0.85 ± 0.09 0.72–1.00 (7)	4.07 ± 0.14 3.77–4.24 (12)	0.71 ± 0.06 0.63–0.81 (11)	2.27 (1)	0.79 ± 0.05 0.71–0.84 (4)	2.14 ± 0.29 1.63–2.58 (11)	1.00 ± 0.05 0.94–1.05 (4)
<i>T. glis</i>	5.51 ± 0.34 4.98–6.24 (30)	0.70 ± 0.08 0.55–0.80 (28)	3.89 ± 0.17 3.49–4.23 (33)	0.67 ± 0.05 0.55–0.79 (28)	2.17 ± 0.20 1.75–2.50 (17)	0.66 ± 0.07 0.54–0.77 (16)	1.90 ± 0.23 1.39–2.35 (29)	0.97 ± 0.09 0.81–1.18 (15)
<i>T. g. discolor</i>	6.58 ± 0.32 6.07–6.93 (5)	0.76 ± 0.01 0.75–0.77 (3)	3.92 ± 0.16 3.68–4.18 (6)	0.69 ± 0.05 0.62–0.75 (4)	2.27 2.20–2.34 (2)	0.64 (1)	1.72 ± 0.29 1.29–2.04 (6)	0.87 ± 0.04 0.83–0.90 (3)
<i>T. g. ferruginea</i>	5.79 ± 0.38 5.10–6.36 (13)	0.74 ± 0.08 0.60–0.85 (11)	4.07 ± 0.25 3.74–4.56 (14)	0.70 ± 0.05 0.64–0.80 (12)	2.29 ± 0.17 2.06–2.53 (11)	0.68 ± 0.04 0.62–0.75 (9)	1.99 ± 0.20 1.62–2.32 (14)	0.97 ± 0.10 0.84–1.15 (7)
<i>T. g. hypochrysa</i>	6.45	0.82	4.13	0.67	—	0.69	2.12	—
<i>T. l. longipes</i>	6.34 ± 0.11 6.23–6.44 (3)	0.84 ± 0.07 0.76–0.89 (3)	4.17 ± 0.13 4.02–4.28 (3)	0.79 ± 0.07 0.73–0.87 (3)	2.39 (1)	0.65 (1)	2.22 (2)	1.00 ± 0.03 0.97–1.02 (3)
<i>T. l. salatana</i>	6.61 ± 0.17 6.46–6.85 (4)	0.83 ± 0.09 0.73–0.89 (3)	4.37 ± 0.15 4.22–4.51 (4)	0.82 ± 0.07 0.78–0.90 (3)	2.41 2.33–2.49 (2)	—	1.86 ± 0.30 1.60–2.19 (3)	1.01 (1)

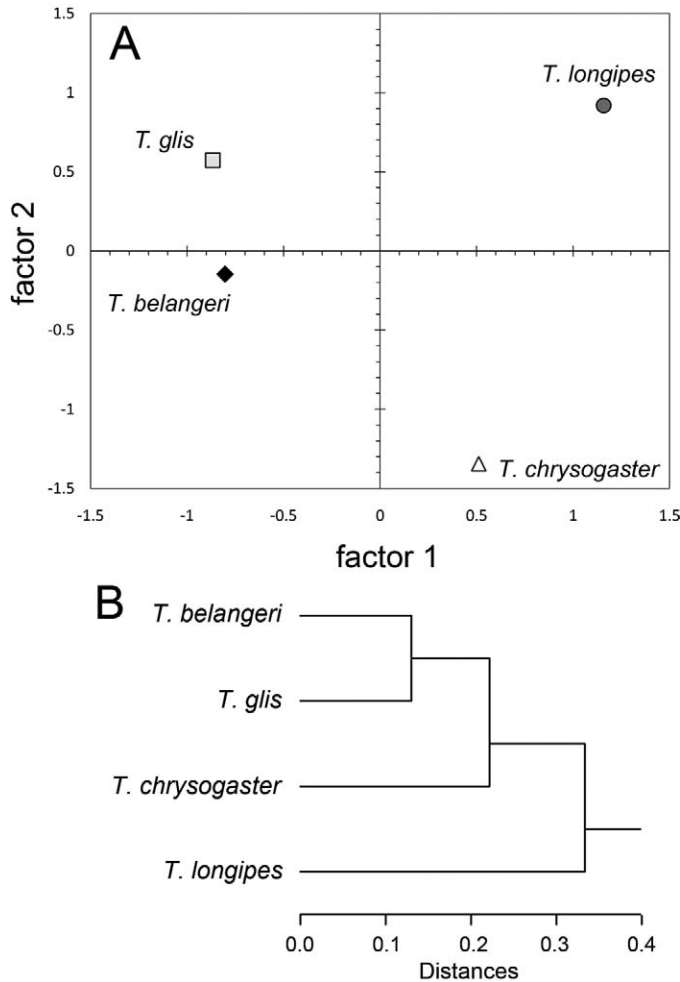


FIG. 3.—Plots illustrating the distinctiveness of 4 currently recognized species, *Tupaia belangeri*, *T. chrysogaster*, *T. glis*, and *T. longipes*. A) Plot of factor scores on first 2 axes from principal components analysis of means of 8 variables from ray IV (Table 3). All 4 taxa plot in different quadrants. B) Phenogram from cluster analysis of 38 variables from all 5 rays.

Five taxa.—In our analyses of 5 taxa (*T. glis*, *T. “glis” discolor*, *T. belangeri*, *T. chrysogaster*, and *T. longipes*), our aim was to determine if the population on Bangka Island designated as *T. “glis” discolor* could be distinguished from the rest of *T. glis*. We again carried out PCA on each ray, but we focus our discussion on ray IV, which provided the greatest separation among the 5 taxa. A bivariate plot of the first 2 factors from the PCA of this ray is shown in Fig. 4A. Factor 1, which accounts for 60% of the total variance, represents size, and factor 2, accounting for 33% of the total variance, is a shape factor representing DPL and PPW contrasted with negatively weighted ML and PPL (Table 4). Along the 1st factor axis, *T. glis*, *T. “glis” discolor*, and *T. belangeri* are about the same size, and they are much smaller than both *T. chrysogaster* and, particularly, *T. longipes*. The 2nd factor axis strongly separates *T. “glis” discolor* from *T. glis* and all of the other species, suggesting that *T. “glis” discolor* averages a

shorter distal phalanx, longer, narrower proximal phalanx, and longer metacarpal.

Plots of PCA scores from the other 4 rays (not shown) exhibit the same general size relationships, except the one for ray III, in which *T. “glis” discolor* has a larger ray than *T. glis*, *T. belangeri*, and *T. chrysogaster*. Regardless of size, the rays of *T. “glis” discolor* are always separated from *T. glis* along the 2nd factor axis.

Our PCA of individuals utilized 10 variables from rays I, III, and IV (Table 5). These variables were chosen because they were complete for all individuals of *T. “glis” discolor*, thereby maximizing sample size for this taxon. Fortunately, this group of variables included a good representation of both lengths and widths of individual bones. In a plot (not shown) of scores on factor axis 1, which represents size (Table 5), and factor axis 2, which contrasts widths and lengths, *T. “glis” discolor* appears as a concentrated subset of *T. glis* in the lower right quadrant. This pattern reflects the medium to large overall size of *T. “glis” discolor* and its long, narrow metacarpals and phalanges relative to the remainder of *T. glis*. In a plot of scores on the 1st and 3rd factor axes (Fig. 4B), *T. “glis” discolor* separates completely from *T. glis* primarily as a result of having long ray I metacarpals contrasted with the lengths of other bones (Tables 2 and 5).

Cluster analysis of 38 variables from these 5 taxa shows that *T. glis* and *T. belangeri* remain most similar to one another, with *T. chrysogaster* as the next most similar species (Fig. 4C). *T. “glis” discolor* is most similar to *T. longipes*, rather than to *T. glis*.

Subspecies of *Tupaia longipes*.—Because of the small sample sizes available, we restricted analyses between *T. l. longipes* and *T. l. salatana* to variables with complete data for all individuals, and the resulting PCA of individual rays had

TABLE 3.—Mean factor scores and component loadings from principal components analysis of 8 variables from ray IV in 4 taxa of *Tupaia* (Fig. 3A). Component loading abbreviations are defined in the “Materials and Methods.” Loadings in boldface type are discussed in the text.

	Axis		
	1	2	3
Mean factor scores			
<i>T. belangeri</i>	−0.80318	−0.14723	−1.25826
<i>T. chrysogaster</i>	0.51114	−1.34401	0.42705
<i>T. glis</i>	−0.86665	0.57233	1.08229
<i>T. longipes</i>	1.15869	0.91891	−0.25108
Component loadings			
4MW	0.986	0.165	0.003
4ML	0.975	0.207	0.083
4MPW	0.961	0.031	−0.276
4PPL	0.915	0.323	0.242
4MPL	0.904	0.408	0.126
4PPW	0.862	−0.226	−0.454
4DPW	0.720	−0.632	0.287
4DPL	0.464	−0.883	0.068
Eigenvalue	5.976	1.573	0.451
% total variance explained	74.7	19.7	5.6

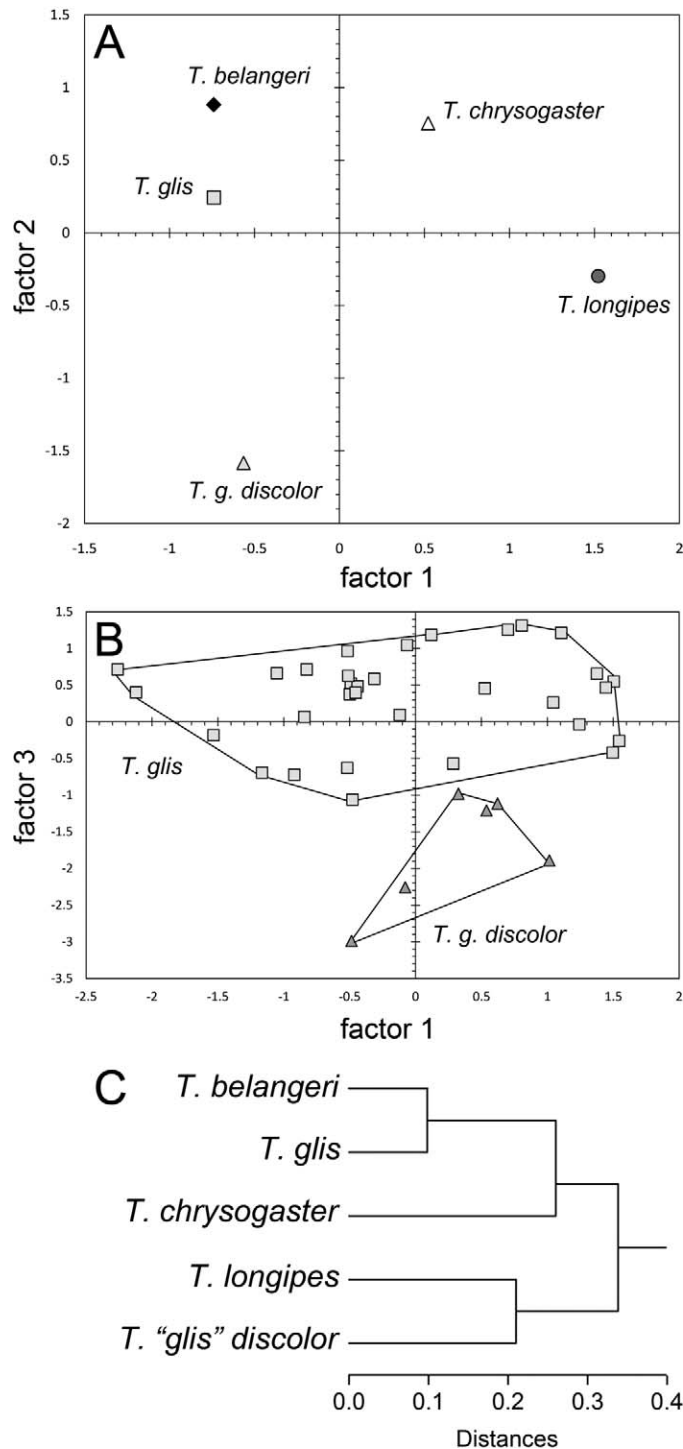


FIG. 4.—Plots illustrating the distinctiveness of *Tupaia* “*glis*” *discolor* from *T. glis*. A) Plot of factor scores on first 2 axes from principal components analysis (PCA) of means of 7 variables from ray IV of 5 taxa, *T. belangeri*, *T. chrysogaster*, *T. glis*, *T. “glis” discolor*, and *T. longipes* (Table 4). *T. “glis” discolor* is in a different quadrant than *T. glis*. B) Plot of factor scores on 1st and 3rd axes from PCA of 10 variables from rays I, III, and IV for individuals of *T. glis* and *T. “glis” discolor* (Table 5). The 2 taxa are well separated from one another. C) Phenogram from cluster analysis of 38 variables from all 5 rays. *T. “glis” discolor* is more similar to *T. longipes* than to *T. glis*.

TABLE 4.—Mean factor scores and component loadings from principal components analysis of 7 variables from ray IV in 5 taxa of *Tupaia* (Fig. 4A). Component loading abbreviations are defined in the “Materials and Methods.” Loadings in boldface type are discussed in the text.

	Axis		
	1	2	3
Mean factor scores			
<i>T. belangeri</i>	−0.74005	0.88211	−0.33756
<i>T. chrysogaster</i>	0.52118	0.75494	1.47139
<i>T. glis</i>	−0.73915	0.24322	−0.82094
<i>T. “glis” discolor</i>	−0.56393	−1.58244	0.55002
<i>T. longipes</i>	1.52195	−0.29783	−0.86291
Component loadings			
4MW	0.933	−0.341	0.085
4MPL	0.931	0.047	−0.308
4MPW	0.889	0.429	−0.107
4PPL	0.775	−0.620	0.041
4PPW	0.705	0.693	−0.078
4ML	0.613	−0.754	0.215
4DPL	0.450	0.772	0.428
Eigenvalue	4.206	2.332	0.351
% total variance explained	60.1	33.3	5.0

only 3 or 4 variables each. In general, the analyses with 4 variables provided clearer separation than those with 3, and we center our discussion on ray I. A bivariate plot of the first 2 factors from the PCA of this ray is shown in Fig. 5A. There is no size factor in this analysis. Instead, factor 1, which accounts for 68% of total variance, is a contrast between the lengths and widths of the metacarpal and proximal phalanx (Table 6). Factor 2, accounting for nearly 15% of the variance, is a shape factor representing MD and PPL. Most of the separation between *T. l. longipes* and *T. l. salata* is along the 1st factor axis. Individual specimens of *T. l. longipes* plot low on this axis, indicating shorter, deeper metacarpals and proximal phalanges than *T. l. salata*. This relationship can be seen just

TABLE 5.—Component loadings from principal components analysis of 10 variables from rays I, III, and IV in individuals of *Tupaia* “*glis*” *discolor* and *T. glis* (Fig. 4B). Component loading abbreviations are defined in the “Materials and Methods.”

	Axis			
	1	2	3	4
Component loadings				
3PPL	0.851	−0.295	−0.316	−0.014
4PPL	0.843	−0.347	−0.223	0.107
1PPW	0.733	0.440	0.006	0.071
1PPL	0.650	0.020	0.402	−0.266
4PPW	0.605	0.618	0.232	−0.029
4MPL	0.599	−0.322	0.538	0.216
3MPL	0.551	−0.288	0.417	−0.240
1ML	0.520	−0.347	−0.640	0.020
3PPW	0.451	0.634	−0.224	0.505
1MW	0.220	0.363	−0.305	−0.793
Eigenvalue	3.946	1.624	1.382	1.077
% total variance explained	39.5	16.2	13.8	10.8

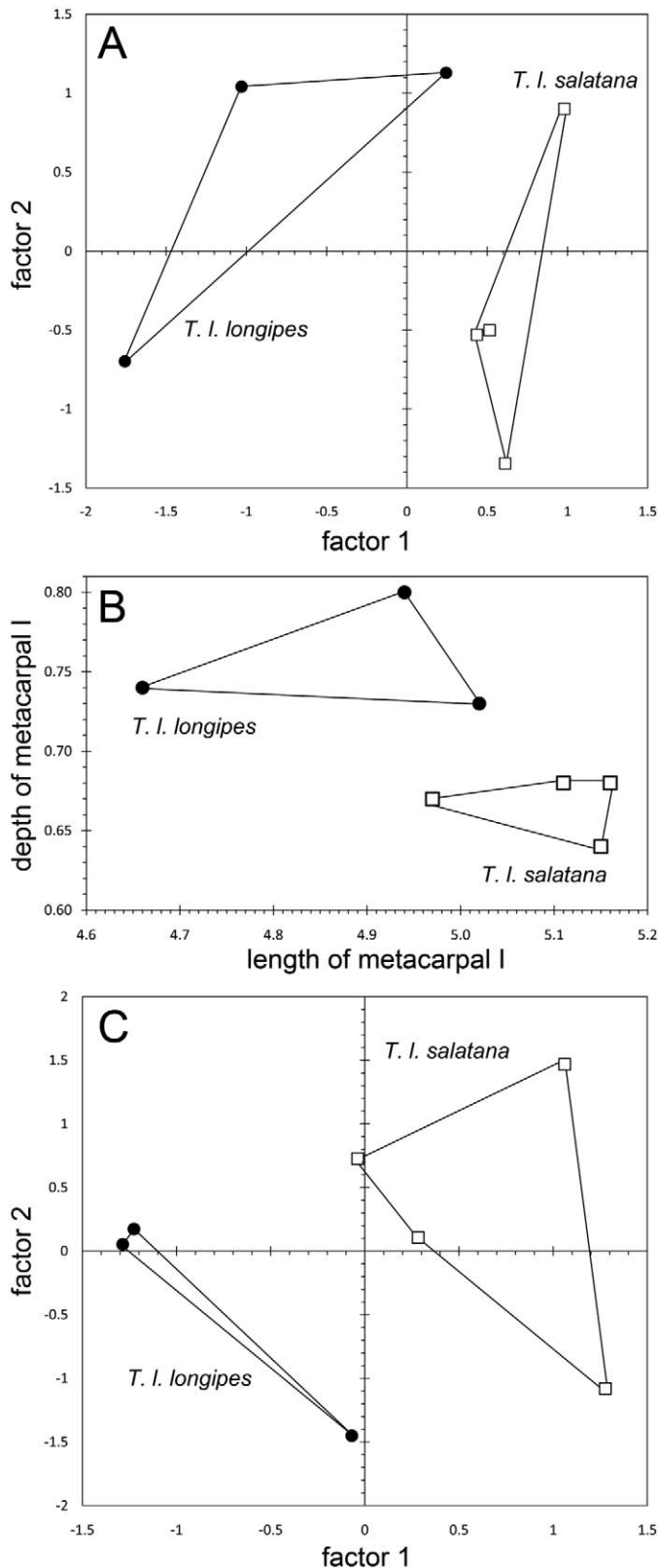


FIG. 5.—Plots illustrating the distinctiveness of *Tupaia longipes* *salatana* from *T. l. longipes*. A) Plot of factor scores on first 2 axes from principal components analysis (PCA) of 4 variables from ray I for individuals of the 2 taxa (Table 6), which are well separated from one another. B) Bivariate plot of metacarpal I length and depth in the 2 taxa. C) Plot of factor scores on first 2 axes from PCA of 10 variables from rays I, IV, and V for individuals of the 2 taxa (Table 7), which are well separated from one another.

TABLE 6.—Factor scores and component loadings from principal components analysis of 4 variables from ray I in *Tupaia longipes longipes* and *T. l. salatana* (Fig. 5A). Component loading abbreviations are defined in the “Materials and Methods.” Loadings in boldface type are discussed in the text.

	Axis		
	1	2	3
Factor scores			
<i>T. l. longipes</i>			
488034	-1.75704	-0.69778	-1.06943
488045	-1.03054	1.04180	1.04074
396673	0.24394	1.12941	0.36524
<i>T. l. salatana</i>			
198040	0.61205	-1.34443	0.41019
198041	0.43596	-0.52928	1.10018
199162	0.51523	-0.50145	-0.39640
198043	0.98039	0.90173	-1.45051
Component loadings			
1PPD	-0.857	-0.237	0.384
1PPL	0.853	0.435	0.098
1ML	0.819	-0.164	0.524
1MD	-0.774	0.568	0.237
Eigenvalue	2.732	0.595	0.488
% total variance explained	68.3	14.9	12.2

as easily in a bivariate plot of metacarpal I length and depth (Fig. 5B). In plots of PCA scores from rays IV and V (not shown), the only other analyses incorporating 4 variables, *T. l. longipes* generally has longer, narrower metacarpals and proximal phalanges than *T. l. salatana*, although the pattern is not as distinct as in the analysis of ray I (Fig. 5A).

A bivariate plot of the first 2 factors from the PCA of 10 variables from rays I, IV, and V is shown in Fig. 5C. Factor 1, which accounts for only 45% of the variance, represents a contrast between the lengths and widths of certain metacarpals and proximal phalanges (Table 7). Factor 2, accounting for more than 28% of the variance, represents the length and width of the 4th metacarpal. Most of the separation between the 2 taxa is along the 1st factor axis, with *T. l. longipes* plotting lower, indicating shorter, wider metacarpals and proximal phalanges than *T. l. salatana*, which plots higher. There is the suggestion of a trend within each taxon of scores decreasing on the 2nd axis as their scores on the 1st axis increase, but sample sizes are too small to fully assess this possible pattern.

Six taxa.—In our analyses of 6 taxa (*T. glis*, *T. “glis” discolor*, *T. belangeri*, *T. chrysogaster*, *T. l. longipes*, and *T. l. salatana*), we carried out PCA on each ray, but we focus our discussion on ray IV, which provided the greatest separation among the 6 taxa. The bivariate plot of the first 2 factors from the PCA of ray IV is shown in Fig. 6A. Factor 1, which accounts for almost 62% of the total variance, represents size, and factor 2, accounting for 31% of the variance, is a shape factor representing DPL and PPW contrasted with negatively weighted ML and PPL (Table 8). There are 3 size groupings along the 1st factor axis: the smallest taxa are represented by *T. glis*, *T. “glis” discolor*, and *T. belangeri*; an intermediate size

TABLE 7.—Factor scores and component loadings from principal components analysis of 10 variables from rays I, IV, and V in *Tupaia longipes longipes* and *T. l. salatana* (Fig. 5C). Component loading abbreviations are defined in the “Materials and Methods.” Loadings in boldface type are discussed in the text.

	Axis		
	1	2	3
Factor scores			
<i>T. l. longipes</i>			
488034	−1.2863	0.05378	−1.32793
488045	−1.2264	0.17403	0.93097
396673	−0.0697	−1.45046	−0.46915
<i>T. l. salatana</i>			
198040	1.06103	1.46815	−0.84617
198041	−0.03798	0.72734	0.27730
199162	0.28278	0.10742	1.53214
198043	1.27649	−1.08026	−0.09715
Component loadings			
4PPW	−0.935	0.148	0.027
1MD	−0.872	−0.297	0.134
1PPD	−0.824	0.394	−0.377
5PPL	0.812	0.118	−0.477
1PPL	0.733	−0.393	0.135
5ML	0.642	0.674	0.030
1ML	0.629	0.310	0.456
4MW	−0.396	0.908	0.103
4ML	0.017	0.904	0.381
4PPL	0.237	0.476	−0.645
Eigenvalues	4.531	2.852	1.187
% total variance explained	45.3	28.5	11.9

group is composed of *T. chrysogaster* and *T. l. salatana*; and the largest taxon is *T. l. longipes*. The greater “size” of *T. l. longipes* compared to *T. l. salatana* in this analysis contrasts with the results from the comparison of just those 2 taxa (see above), in which *T. l. salatana* appeared to be larger. The difference is attributable to the higher loadings of width variables on the 1st axis in this analysis (Table 8) versus the higher loadings of length variables in the previous set of analyses (Table 7). The 2nd factor axis in this analysis clearly separates *T. glis*, *T. belangeri*, *T. chrysogaster*, and *T. l. longipes*, which have positive scores on this axis (representing the possession of a relatively long distal phalanx; short metacarpal; and short, wide proximal phalanx), from *T. “glis” discolor* and *T. l. salatana*, which have strongly negative scores (a result of relatively short distal phalanges; long metacarpals; and long, narrow proximal phalanges). Plots of PCA scores from the other 4 rays (not shown) exhibit generally similar size relationships, but degrees of separation along the 2nd factor axis vary.

Cluster analysis of 38 variables from these 6 taxa shows 2 distinct subsets composed of 3 taxa each (Fig. 6B). In 1 subset, *T. glis* is most similar to *T. belangeri*, with *T. chrysogaster* as the next most similar species. In the 2nd subset, *T. “glis” discolor* is most similar to *T. l. salatana*, with *T. l. longipes* as the next most similar taxon.

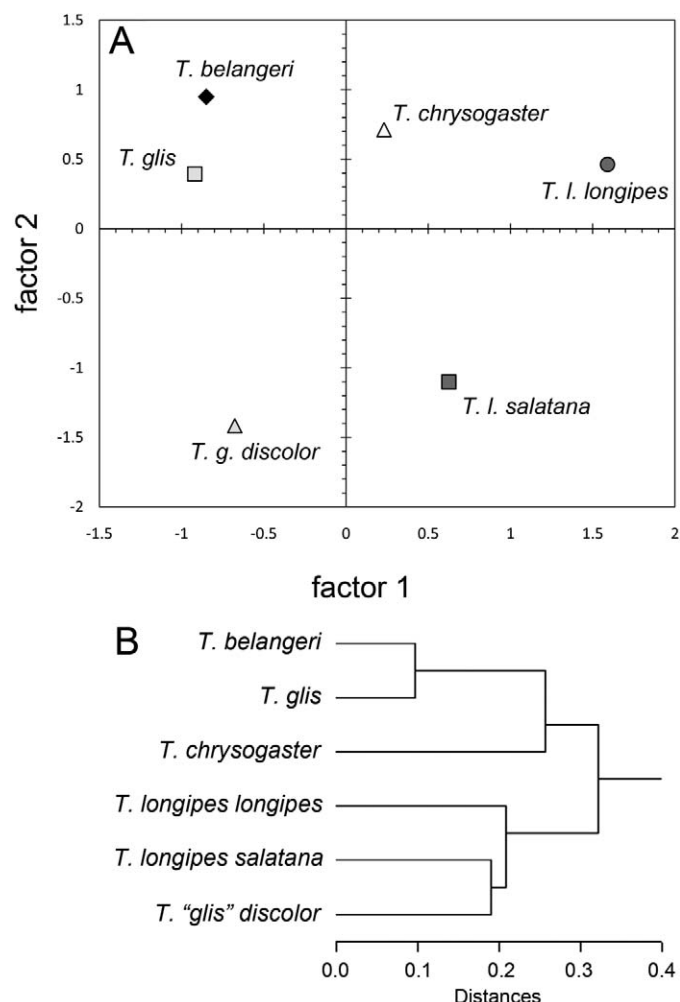


FIG. 6.—Plots illustrating the distinctiveness of *Tupaia longipes salatana* from *T. l. longipes*. A) Plot of factor scores on first 2 axes from principal components analysis of means of 7 variables from ray IV of 6 taxa, *T. belangeri*, *T. chrysogaster*, *T. glis*, *T. “glis” discolor*, *T. longipes longipes*, and *T. l. salatana* (Table 8). *T. l. longipes* and *T. l. salatana* are in different quadrants. B) Phenogram from cluster analysis of 38 variables from all 5 rays. *T. l. salatana* is more similar to *T. “glis” discolor* than to *T. l. longipes*.

Seven taxa.—In our analyses of 7 taxa (*T. glis*, *T. “glis” discolor*, *T. “glis” ferruginea*, *T. belangeri*, *T. chrysogaster*, *T. l. longipes*, and *T. l. salatana*), our aim was to test whether the population from Sumatra designated as *T. “glis” ferruginea* could be distinguished from the rest of *T. glis*. We carried out PCA on each ray, but we focus our discussion on rays I and II, which provided the greatest separation among the 7 taxa. A bivariate plot of the first 2 factors from the PCA of ray I is shown in Fig. 7A. The 1st factor axis, which represents 56% of the total variance, is a size vector, but with minor contributions from DPD and ML (Table 9). Along this axis, there are 4 general size groupings, from smallest to largest: *T. glis*, *T. belangeri*, and *T. “glis” discolor*; *T. “glis” ferruginea*; *T. l. salatana* and *T. chrysogaster*; and *T. l. longipes*. The 2nd factor axis, comprising 27% of the variance, represents DPD and ML. This axis separates *T. “glis” discolor*, with its longer

TABLE 8.—Mean factor scores and component loadings from principal components analysis of 7 variables from ray IV in 6 taxa of *Tupaia* (Fig. 6A). Component loading abbreviations are defined in the “Materials and Methods.” Loadings in boldface type are discussed in the text.

	Axis		
	1	2	3
Mean factor scores			
<i>T. belangeri</i>	−0.85033	0.94927	−0.56684
<i>T. chrysogaster</i>	0.23127	0.71238	1.80683
<i>T. glis</i>	−0.91979	0.39443	−0.72864
<i>T. “glis” discolor</i>	−0.67674	−1.41687	0.55795
<i>T. longipes longipes</i>	1.59001	0.46271	−0.54286
<i>T. l. salatana</i>	0.62557	−1.10191	−0.52643
Component loadings			
4MPW	0.912	0.341	−0.078
4MW	0.899	−0.408	0.053
4MPL	0.894	0.187	−0.240
4PPW	0.798	0.579	−0.092
4PPL	0.791	− 0.598	0.032
4ML	0.631	− 0.747	0.175
4DPL	0.470	0.789	0.375
Eigenvalue	4.321	2.192	0.247
% total variance explained	61.7	31.3	3.5

metacarpal and deeper distal phalanx, from *T. glis*, *T. “glis” ferruginea*, and *T. belangeri*. To a lesser degree, it also separates *T. l. salatana* and *T. l. longipes*.

In the bivariate plot of the first 2 factors from the PCA of ray II (Fig. 7B), the 1st factor axis is a size vector representing 50% of the total variance, but with little to no contribution from DPL, DPW, or MPL (Table 10). As in the plot from the PCA of ray I, there are 4 size groupings in this plot, but the order of taxa and the memberships of the size groupings are different. From smallest to largest, the groupings are: *T. glis* and *T. belangeri*; *T. “glis” ferruginea* and *T. “glis” discolor*; *T. chrysogaster*; and *T. l. salatana* and *T. l. longipes*. The 2nd factor axis, which comprised nearly 30% of the total variance, represents DPL and DPW. This axis better distributes the groupings by separating those taxa with longer and wider distal phalanges (i.e., *T. glis*, *T. belangeri*, *T. chrysogaster*, and *T. l. longipes*) from those with a shorter, narrower distal phalanx (*T. “glis” ferruginea*, *T. “glis” discolor*, and *T. l. salatana*).

The middle 3 rays exhibit the same general size relationships among the 7 taxa. Plots of PCA scores from rays III and IV (not shown) show the same relative size rankings along the 1st factor axis as those for ray II (Fig. 7B), with the exceptions that *T. “glis” discolor* averages a smaller ray IV than *T. “glis” ferruginea*, and *T. chrysogaster* averages a smaller ray III than *T. “glis” discolor*. In all 3 cases, the smallest rays are those of *T. glis* and the largest are those of *T. l. longipes*. The plot for ray V (not shown) is distinct in that this ray is smaller in *T. “glis” discolor* than in *T. belangeri*, and that of *T. l. salatana* is larger than that of *T. l. longipes*.

In our analyses of individuals of *T. “glis” ferruginea* and *T. glis*, we initially used all remaining subspecies of *T. glis* to represent that species. One outlier, however, skewed the results by greatly increasing the area on our plots occupied by *T. glis*.

The specimen was the sole representative of the subspecies *T. “glis” hypochrysa*, the only representative of *T. glis* from Java, and one we ultimately tested for its distinctiveness (see below). In the results presented here, this taxon is not included in the analysis. Our PCA of individuals used 10 variables from all 5 rays (Table 11), chosen primarily because they were complete for all individuals of *T. “glis” ferruginea*, thereby obtaining the maximum available sample size for this taxon. In a plot of scores on the first 2 factor axes (Fig. 7C), most individuals of *T. “glis” ferruginea* plot toward the upper right-hand quadrant, outside the large region circumscribed by *T. glis*. This position reflects the overall larger size (factor 1) and relatively narrower rays (factor 2) of *T. “glis” ferruginea*. There is some overlap with *T. glis*, however, and the 3 smallest individuals of *T. “glis” ferruginea* nest well within the plot for that species. We should note here that our subsequent analyses that focused on investigating the potential distinctiveness of *T. “glis” hypochrysa* used a 4-taxon model that included *T. “glis” ferruginea* (see below). In those analyses, *T. “glis” ferruginea* is even further removed from *T. glis* (Fig. 8).

Cluster analysis of 38 variables shows 3 main groupings of taxa based on similarity of the hand bones (Fig. 7D). *T. glis* remains most similar to *T. belangeri*. This pairing is most similar to the pairing of *T. “glis” ferruginea* and *T. chrysogaster*. The 3rd grouping is composed of 3 species, with *T. “glis” discolor* most similar to *T. l. salatana*, and this pairing most similar to *T. l. longipes*.

Javan Tupaia “glis” hypochrysa.—In our analyses of the potential distinctiveness of Javan *T. “glis” hypochrysa* relative to *T. chrysogaster*, *T. glis*, and *T. “glis” ferruginea*, we conducted PCA on each ray, but we focus our discussion on ray IV, which provided the greatest separation among the 4 groups. The bivariate plot of the first 2 factors from the PCA of ray IV is shown in Fig. 8A. The 1st factor axis accounts for more than 80% of the total variance and is a size vector, whereas the 2nd factor axis, accounting for 13% of the variance, is DPL contrasted with negatively weighted MPL and PPL (Table 12). In this plot, the 4 groups segregate into the 4 quadrants. Size relationships show *T. glis* as having the smallest ray IV, followed in order by *T. “glis” ferruginea*, *T. chrysogaster*, and *T. “glis” hypochrysa* with the largest. Along the 2nd factor axis, *T. “glis” ferruginea* has relatively long proximal and middle phalanges, but short distal phalanges; *T. glis* and *T. “glis” hypochrysa* are intermediate, although the former has a positive score and the latter a negative one; and *T. chrysogaster* has relatively short proximal and middle phalanges, but long distal phalanges. The size relationships hold for rays II and III as well, but *T. chrysogaster* has a larger ray V than *T. “glis” hypochrysa* and both *T. chrysogaster* and *T. “glis” ferruginea* have a larger ray I. *T. glis* always exhibits the smallest rays.

In our analysis of individuals, the PCA model included 5 variables from ray IV (Table 13). The 1st factor axis in this analysis represents overall size of ray IV, and the 2nd axis is MPL contrasted with a negatively weighted DPL (with some contribution from PPW). In a plot of these first 2 factors (Fig.

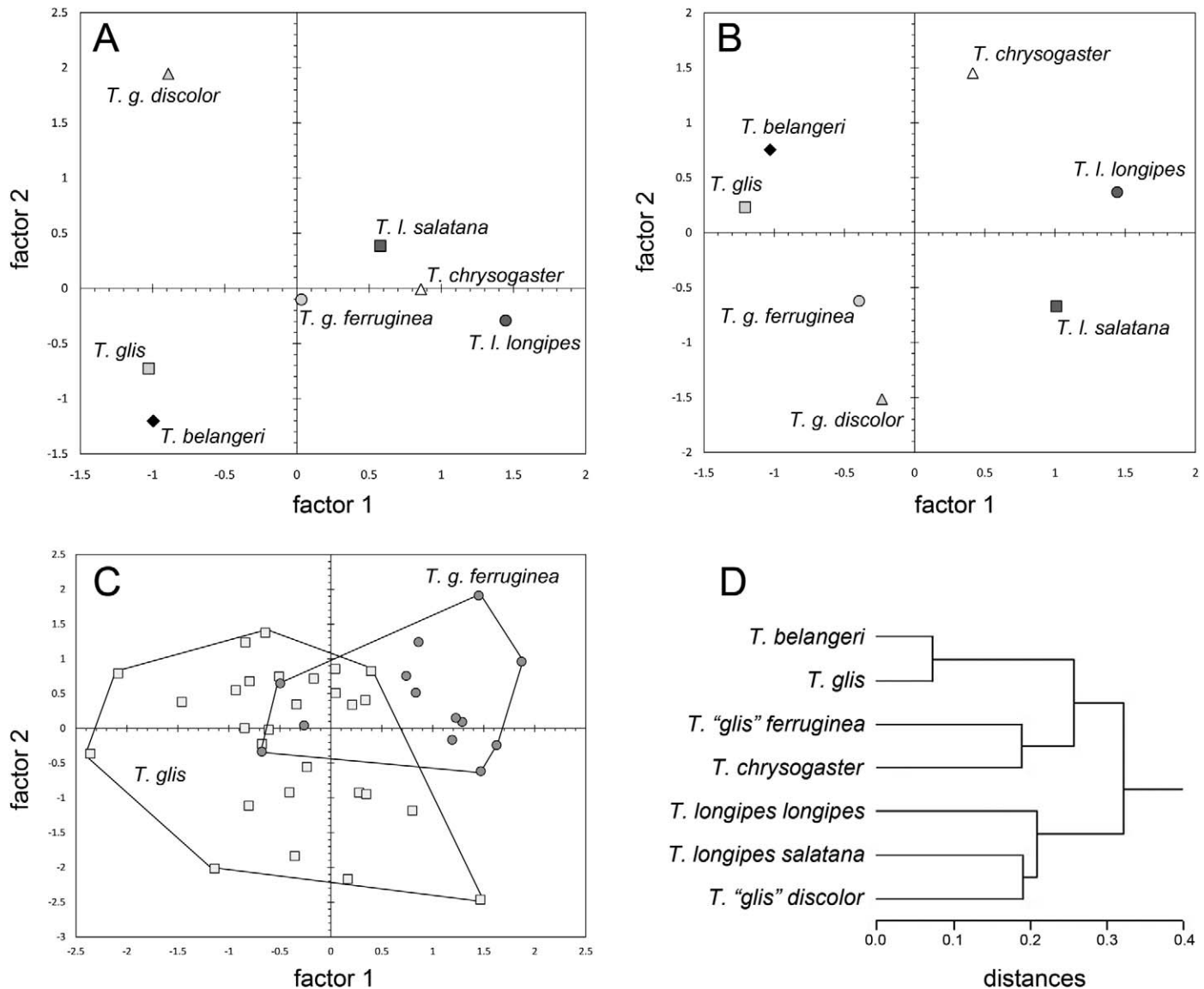


FIG. 7.—Plots illustrating the distinctiveness of *Tupaia* "glis" *ferruginea* from *T. glis*. Plots of factor scores on first 2 axes from principal components analysis (PCA) of means of 7 taxa (*T. belangeri*, *T. chrysogaster*, *T. glis*, *T. "glis" ferruginea*, *T. "glis" discolor*, *T. longipes longipes*, and *T. l. salatana*) for A) 6 variables from ray I (Table 9) and B) 8 variables from ray II (Table 10). *T. "glis" ferruginea* and *T. glis* are well separated from one another. C) Plot of factor scores on first 2 axes from a PCA of 10 variables from all 5 rays for individuals of *T. glis* and *T. "glis" ferruginea* (Table 11). See also Fig. 8B. D) Phenogram from cluster analysis of 38 variables from all 5 rays. *T. "glis" ferruginea* is more similar to *T. chrysogaster* than to *T. glis*.

8B), *T. glis* has the smallest components of ray IV and *T. chrysogaster* and *T. "glis" ferruginea* are intermediate in size, although both overlap with the largest *T. glis* on the 1st axis. The single specimen of *T. "glis" hypochrysa* has by far the largest ray IV, and it is well separated from the other 3 taxa. *T. chrysogaster*, *T. "glis" hypochrysa*, and *T. "glis" ferruginea* all mostly overlap the broad range of *T. glis* along the 2nd axis, although the largest individuals (i.e., those with the longest MPL and shortest DPL) are *T. "glis" ferruginea*. This axis mostly separates *T. "glis" ferruginea* from *T. chrysogaster*. A combination of the 2 axes separates *T. "glis" ferruginea* from *T. glis*.

Cluster analysis of 31 variables from these 4 taxa shows that *T. chrysogaster* and *T. "glis" ferruginea* are most similar to one another (Fig. 8C), although there is a substantial distance between them. The next most similar taxon to that group is *T. "glis" hypochrysa*. *T. glis* is the least similar to the other 3 taxa in this analysis, although the distance separating them is small.

DISCUSSION

Taxonomic implications.—*Tupaia glis* has long been used as a "wastebasket" taxon, and it currently includes 27 synonyms (Helgen 2005). In our study, we initially set out to assess the distinctiveness of hand proportions among 4

TABLE 9.—Mean factor scores and component loadings from principal components analysis of 6 variables from ray I in 7 taxa of *Tupaia* (Fig. 7A). Component loading abbreviations are defined in the “Materials and Methods.” Loadings in boldface type are discussed in the text.

	Axis		
	1	2	3
Mean factor scores			
<i>T. belangeri</i>	−0.99462	−1.20237	−0.06838
<i>T. glis</i>	−1.02718	−0.72657	0.18332
<i>T. “glis” ferruginea</i>	0.03072	−0.10112	−0.41419
<i>T. “glis” discolor</i>	−0.89101	1.94504	0.35648
<i>T. chrysogaster</i>	0.85879	−0.00819	1.64030
<i>T. longipes longipes</i>	1.44545	−0.29148	0.02638
<i>T. l. salataana</i>	0.57785	0.38468	−1.72390
Component loadings			
1PPD	0.987	0.014	0.056
1MD	0.952	0.068	0.124
1DPL	0.812	−0.489	0.299
1PPL	0.708	−0.401	−0.434
1DPD	0.277	0.814	0.327
1ML	0.498	0.757	−0.400
Eigenvalue	3.367	1.639	0.563
% total variance explained	56.1	27.3	9.4

species of treeshrews previously considered as part of a more inclusive *T. glis* but now recognized as distinct species. The results of our analyses support the separation of these 4 species and demonstrate the potential utility of hand proportions in distinguishing closely related species of treeshrews. We further explored this method using other

TABLE 10.—Mean factor scores and component loadings from principal components analysis of 8 variables from ray II in 7 taxa of *Tupaia* (Fig. 7B). Component loading abbreviations are defined in the “Materials and Methods.” Loadings in boldface type are discussed in the text.

	Axis		
	1	2	3
Mean factor scores			
<i>T. belangeri</i>	−1.02907	0.75388	−1.25620
<i>T. glis</i>	−1.20828	0.23109	−0.24836
<i>T. “glis” ferruginea</i>	−0.39560	−0.62229	1.12581
<i>T. “glis” discolor</i>	−0.23270	−1.51417	0.23175
<i>T. chrysogaster</i>	0.41402	1.45360	1.44526
<i>T. longipes longipes</i>	1.44237	0.36843	−0.88111
<i>T. l. salataana</i>	1.00926	−0.67054	−0.41714
Component loadings			
2MPW	0.968	0.073	−0.023
2PPW	0.889	0.315	−0.278
2PPL	0.889	−0.311	0.171
2MW	0.889	0.313	0.135
2ML	0.840	−0.459	−0.064
2DPL	0.105	0.981	0.026
2DPW	− 0.037	0.824	0.563
2MPL	0.080	−0.488	0.857
Eigenvalue	4.032	2.390	1.182
% total variance explained	50.4	29.9	14.8

TABLE 11.—Component loadings from principal components analysis of 10 variables from all 5 rays in individuals of *Tupaia “glis” ferruginea* and *T. glis* (Fig. 7C). Component loading abbreviations are defined in the “Materials and Methods.”

	Axis		
	1	2	3
Component loadings			
2PPL	0.919	0.016	0.102
3PPL	0.915	0.015	0.091
4PPL	0.889	0.141	0.198
1PPL	0.856	0.064	−0.163
1ML	0.767	0.328	−0.385
2ML	0.763	0.127	−0.396
5PPL	0.743	0.226	0.331
1PPW	0.683	−0.567	0.159
3PPW	0.368	−0.768	0.246
1MW	0.098	−0.578	−0.624
Eigenvalue	5.540	1.445	0.976
% total variance explained	55.4	14.5	9.8

geographically circumscribed populations for which we had adequate samples.

The results of our analyses of populations of purported *T. glis* from Bangka Island (*T. “glis” discolor*) and Sumatra (*T. “glis” ferruginea*) show these 2 forms to have manus proportions distinct from those of mainland peninsular *T. glis* (see Fig. 9 for ranges). Recognition of *T. discolor* and *T. ferruginea* as distinct species will be further tested in molecular phylogeographic and craniodental morphometric analyses of *T. glis*, *T. chrysogaster*, *T. longipes*, and *T. belangeri*. *T. discolor* is further distinguished from *T. glis* based on mammae count and absence of the entepicondylar foramen of the humerus (Table 1; Lyon 1913). The separation of these island taxa from *T. glis* greatly reduces its geographic distribution, restricting *T. glis* primarily to the Malay Peninsula (south of the Isthmus of Kra) and surrounding islands (Fig. 9).

Tupaia longipes and *T. salataana* from Borneo (Fig. 9) have long been considered distinct as northern and southern subspecies (e.g., Helgen 2005; Lyon 1913), but our study shows that their substantial difference in manus proportions is equal to that found between recognized species. Although this distinction certainly requires comprehensive testing with larger samples and additional types of data (e.g., molecular and craniodental), we are sufficiently confident in our results to consider them distinct species.

Our analyses of manus proportions in *T. “glis” hypochrysa* from Java (Fig. 9) strongly suggest that this island taxon, like those from intervening Bangka Island and Sumatra, is distinct from peninsular Malaysian *T. glis*. Although this makes sense on geographical grounds, the small sample available to us combined with the lack of other morphological or molecular studies providing supporting evidence prevents us from formally recognizing *T. hypochrysa* as a distinct species at this time. Our results, should, however, be a signal that the systematics of this population warrant further testing in future molecular and morphological analyses.

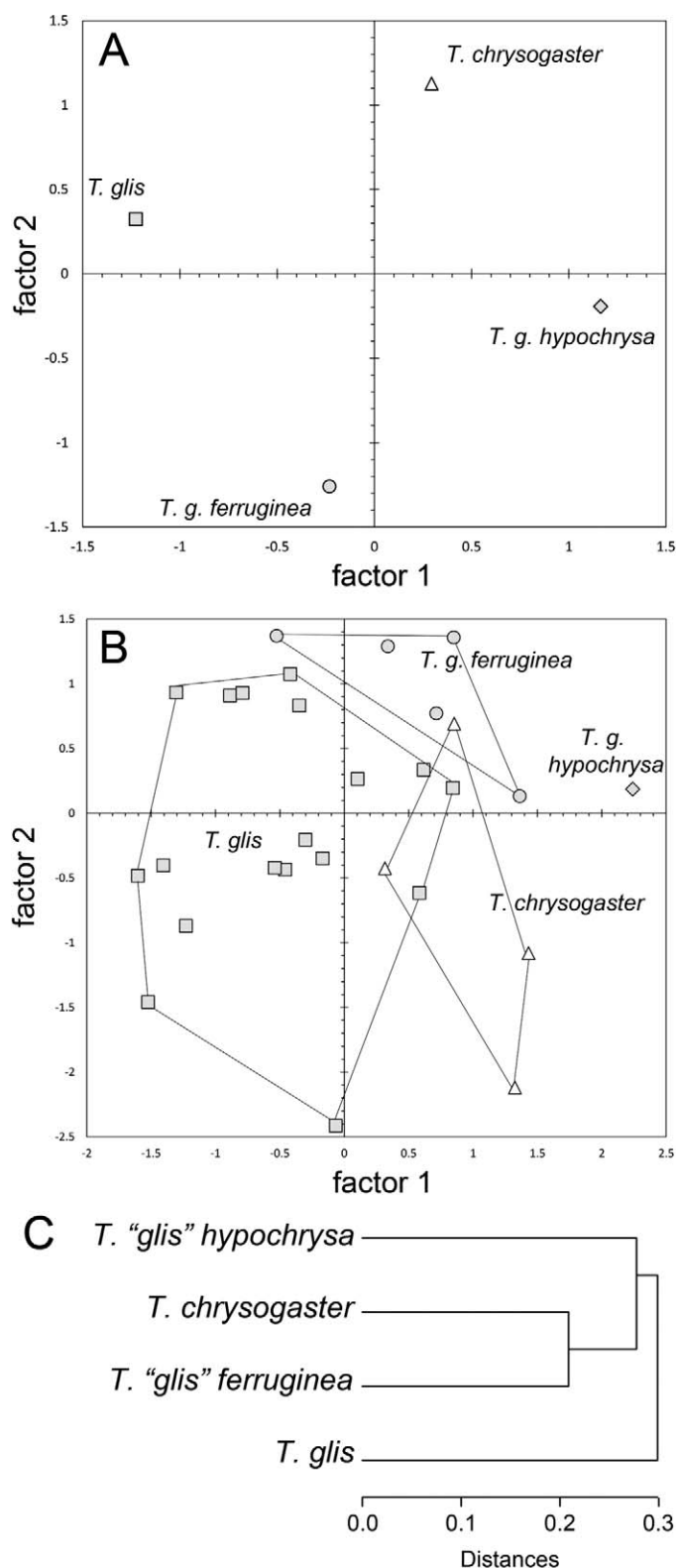


FIG. 8.—Plots illustrating the distinctiveness of *Tupaia* “*glis*” *hypochrysa* relative to *T. chrysogaster*, *T. glis*, and *T. “glis” ferruginea*. A) Plot of factor scores on first 2 axes from principal components analysis (PCA) of means of 6 variables from ray IV (Table 12). All 4 taxa plot in different quadrants. B) Plot of factor scores on first 2 axes from PCA of 5 variables from ray IV for individuals (Table 13). *T. “glis” hypochrysa* is distinct from the other 3 taxa. C) Phenogram from cluster analysis of 31 variables from all 5 rays. *T. “glis” hypochrysa* is more similar to *T. chrysogaster* and *T. “glis” ferruginea* than to *T. glis*.

TABLE 12.—Mean factor scores and component loadings from principal components analysis of 6 variables from ray IV in *Tupaia glis*, *T. chrysogaster*, *T. g. ferruginea*, and *T. g. hypochrysa* (Fig. 8A). Component loading abbreviations are defined in the “Materials and Methods.” Loadings in boldface type are discussed in the text.

	Axis		
	1	2	3
Mean factor scores			
<i>T. chrysogaster</i>	0.29442	1.12811	−0.94377
<i>T. g. ferruginea</i>	−0.23123	−1.25886	−0.78219
<i>T. g. hypochrysa</i>	1.16378	−0.19358	0.92636
<i>T. glis</i>	−1.22697	0.32433	0.79959
Component loadings			
4ML	0.996	0.088	−0.012
4PPW	0.967	0.182	0.179
4PPL	0.944	−0.315	0.093
4MPL	0.857	−0.487	0.169
4MPW	0.829	−0.043	−0.557
4DPL	0.768	0.634	0.089
Eigenvalue	4.831	0.781	0.38
% total variance explained	80.5	13.0	6.5

Our analysis of hand proportions provides strong morphological evidence that supports recognition of 3 additional species of *Tupaia* in Indonesia (Fig. 9). Given the 15 (Helgen 2005) or 16 (Roberts et al. 2011) species of *Tupaia* currently recognized, this is a considerable addition to the diversity of this genus and contributes to our understanding of the diversity of this geographic region. The distribution of these species on islands in the Indonesian archipelago has serious conservation implications for these relatively small, potentially vulnerable populations.

Conservation implications.—Efforts to identify conservation priorities for treeshrews are severely compromised by taxonomic instability (e.g., all treeshrew species are currently listed in Appendix II of the Convention on International Trade in Endangered Species of Wild Fauna and Flora [CITES; e.g., Han 2008; Meijaard and MacKinnon 2008]). Helgen (2005:104) qualified his treeshrew chapter in the 3rd edition of *Mammal Species of the World* as “no substitute for a

TABLE 13.—Component loadings from principal components analysis of 5 variables from ray IV in individuals of *Tupaia glis*, *T. chrysogaster*, *T. g. ferruginea*, and *T. g. hypochrysa* (Fig. 8B). Component loading abbreviations are defined in the “Materials and Methods.” Loadings in boldface type are discussed in the text.

	Axis		
	1	2	3
Component loadings			
4PPL	0.869	0.255	0.036
4ML	0.848	0.069	0.406
4MPL	0.638	0.578	−0.250
4PPW	0.566	−0.465	−0.659
4DPL	0.550	−0.702	0.285
Eigenvalue	2.505	1.112	0.744
% total variance explained	50.1	22.2	14.9

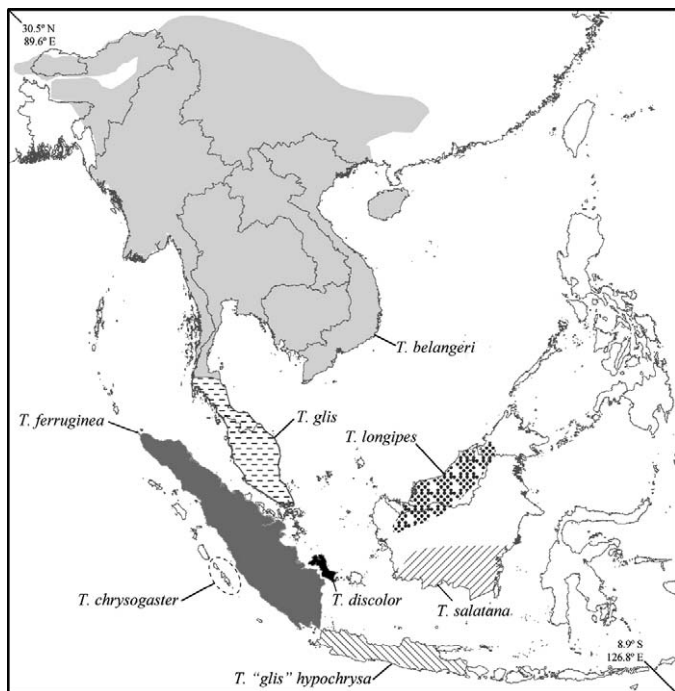


FIG. 9.—Map of Southeast Asia showing approximate ranges of 8 treeshrew taxa, including 3 species resurrected here (*Tupaia ferruginea*, *T. discolor*, and *T. salatana*). Note the revised range of *T. glis*, including *T. "glis" hypochrysa*. Map is redrawn from Roberts et al. (2011: figure 1) and Lyon (1913:75).

comprehensive systematic review of the order.” Only when the taxonomy of Scandentia has been revised with modern molecular and morphological methods will it be possible to seriously address treeshrew conservation priorities (Olson et al. 2004a; Schlick-Steiner et al. 2007). Treeshrews are distributed in 3 of the world’s foremost biodiversity hotspots: Sundaland, Indo-Burma, and the Philippines (Myers et al. 2000). Although Southeast Asia is on the threshold of a biodiversity disaster, there is a paucity of data for conservation efforts on even the more frequently studied taxa from these 3 hotspots (Sodhi et al. 2004). Sundaland in particular is among the 5 richest hotspots that house 16% of all the world’s vertebrates on 0.4% of the earth’s surface (Myers et al. 2000), yet there are fewer biodiversity-related publications concerning this and other Southeast Asian regions than for less-distressed areas (Sodhi et al. 2004). Hence, any taxonomic revision of poorly studied taxa from Southeast Asia, such as treeshrews, could have major implications for conservation strategies of those taxa.

The case of *T. chrysogaster* illustrates the continued relevance of taxonomic revision on the conservation status of a species. Most treeshrews are classified as species of “Least Concern” on the *IUCN Red List of Threatened Species* (e.g., Han 2008), whereas the island endemic *T. chrysogaster* is 1 of only 2 species considered to be endangered (Meijaard and MacKinnon 2008). The resurrection of this species by Wilson (1993) was critical for accurately assessing the conservation status of the population on the Mentawai Islands (Fig. 9),

which otherwise would have been overlooked as part of a widespread *T. glis*. Similarly, our recognition of *T. ferruginea* from Sumatra and *T. salatana* and *T. longipes* from Borneo should focus greater attention on those populations. More closely analogous to the case of *T. chrysogaster* is that of *T. discolor* from Bangka Island (Fig. 9), which is much smaller in area than Sumatra or Borneo, although certainly larger than the 3 Mentawai Islands in which *T. chrysogaster* is distributed (i.e., North and South Pagai Islands and Sipora; Fig. 9). Recognition of *T. discolor* necessitates a reassessment of its conservation status. Moreover, the removal of these populations from *T. glis* reduces its effective geographic range, warranting a reevaluation of its status as well. Given such conservation implications, the taxonomic boundaries of problematic taxa such as the *T. glis*–*T. belangeri* species complex must continue to be explored with additional molecular and morphological evidence. And, as this study shows, morphological analyses should not be restricted to traditional craniodental or external measurements, but expanded to include postcranial data as well.

ACKNOWLEDGMENTS

This research was supported by National Science Foundation grant DEB-0542532/0542725 and an Alaska EPSCoR grant to EJS and LEO. Additional support was provided to NW from the United States Geological Survey’s Patuxent Wildlife Research Center. We are grateful to S. Raredon, Division of Fishes, Museum Support Center, USNM, for help with the digital X-ray system. This manuscript was completed when LEO was supported by an Edward P. Bass Distinguished Visiting Environmental Scholarship from the Yale Institute for Biospheric Studies. Any use of trade, product, or firm names is for descriptive purposes only and does not imply endorsement by the United States government. We thank R. M. Timm and an anonymous reviewer for comments that improved the manuscript.

LITERATURE CITED

- BLOCH, J. I., M. T. SILCOX, D. M. BOYER, AND E. J. SARGIS. 2007. New Paleocene skeletons and the relationship of plesiadapiforms to crown-clade primates. *Proceedings of the National Academy of Sciences* 104:1159–1164.
- BUTLER, P. M. 1972. The problem of insectivore classification. Pp. 253–265 in *Studies in vertebrate evolution* (K. A. Joysey and T. S. Kemp, eds.). Oliver and Boyd, Edinburgh, Scotland.
- CARLSSON, A. 1922. Über die Tupaiidae und ihre Beziehungen zu den Insectivora und den Prosimiae. *Acta Zoologica*, Stockholm 3:227–270.
- CARROLL, R. L. 1988. *Vertebrate paleontology and evolution*. W. H. Freeman, New York.
- CHASEN, F. N. 1940. A handlist of Malaysian mammals. *Bulletin of the Raffles Museum*, Singapore 15:1–209.
- CORBET, G. B., AND J. E. HILL. 1980. *A world list of mammalian species*. British Museum (Natural History), London, United Kingdom.
- CORBET, G. B., AND J. E. HILL. 1992. *The mammals of the Indomalayan region: a systematic review*. Oxford University Press, Oxford, United Kingdom.

- DENE, H., M. GOODMAN, AND W. PRYCHODKO. 1978. An immunological examination of the systematics of Tupaioidea. *Journal of Mammalogy* 59:697–706.
- DENE, H., M. GOODMAN, W. PRYCHODKO, AND G. MATSUDA. 1980. Molecular evidence for the affinities of Tupaiidae. Pp. 269–291 in *Comparative biology and evolutionary relationships of tree shrews* (W. P. Luckett, ed.). Plenum, New York.
- DIARD, P. M. 1820. Report of a meeting of the Asiatic Society for March 10. *Asiatic Journal and Monthly Register* 10:477–478.
- DUFF, A., AND A. LAWSON. 2004. *Mammals of the world: a checklist*. Yale University Press, New Haven, Connecticut.
- EMMONS, L. H. 2000. *Tupaia: a field study of Bornean treeshrews*. University of California Press, Berkeley.
- ENDO, H., ET AL. 2000a. Multivariate analysis in skull osteometry of the common tree shrew from both sides of the Isthmus of Kra in southern Thailand. *Journal of Veterinary Medical Science* 62:375–378.
- ENDO, H., ET AL. 2000b. Sympatric distribution of the two morphological types of the common tree shrew in Hat-Yai districts (South Thailand). *Journal of Veterinary Medical Science* 62:759–761.
- ESSER, D., S. SCHEHKA, AND E. ZIMMERMANN. 2008. Species-specificity in communication calls of tree shrews (*Tupaia*: Scandentia). *Journal of Mammalogy* 89:1456–1463.
- HAN, K.-H. 2008. *Tupaia glis*. In: IUCN 2011. IUCN Red list of threatened species. Version 2011.1. www.iucnredlist.org. Accessed 20 August 2011.
- HAN, K.-H., F. H. SHELDON, AND R. B. STUEBING. 2000. Interspecific relationships and biogeography of some Bornean tree shrews (Tupaidae: *Tupaia*), based on DNA hybridization and morphometric comparisons. *Biological Journal of the Linnean Society* 70:1–14.
- HELGEN, K. M. 2005. Order Scandentia. Pp. 104–109 in *Mammal species of the world: a taxonomic and geographic reference* (D. E. Wilson and D. M. Reeder, eds.). 3rd ed. Johns Hopkins University Press, Baltimore, Maryland.
- HILL, J. E. 1960. The Robinson collection of Malaysian mammals. *Bulletin of the Raffles Museum, Singapore* 29:1–112.
- HIRAI, H., Y. HIRAI, Y. KAWAMOTO, H. ENDO, J. KIMURA, AND W. RERKAMNUAYCHOKE. 2002. Cytogenetic differentiation of two sympatric tree shrew taxa found in the southern part of the Isthmus of Kra. *Chromosome Research* 9:313–327.
- HONACKI, J. H., K. E. KINMAN, AND J. W. KOEPL. 1982. *Mammal species of the world: a taxonomic and geographic reference*. 1st ed. Allen Press, Inc., Lawrence, Kansas.
- JANECKA, J., ET AL. 2007. Molecular and genomic data identify the closest living relative of primates. *Science* 318:792–794.
- KARDONG, K. V. 1998. *Vertebrates: comparative anatomy, function, evolution*. WCB McGraw-Hill, New York.
- KAWAMICHI, T., AND M. KAWAMICHI. 1979. Spatial organization and territory of tree shrews (*Tupaia glis*). *Animal Behaviour* 27:381–393.
- KIRK, E. C., P. LEMELIN, M. W. HAMRICK, D. M. BOYER, AND J. I. BLOCH. 2008. Intrinsic hand proportions of euarchontans and other mammals: implications for the locomotor behavior of plesiadapiforms. *Journal of Human Evolution* 55:278–299.
- LANGHAM, N. P. E. 1982. The ecology of the common tree shrew *Tupaia glis* in peninsular Malaysia. *Journal of Zoology (London)* 197:323–344.
- LIU, L., L. YU, D. K. PEARL, AND S. V. EDWARDS. 2009. Estimating species phylogenies using coalescence times among sequences. *Systematic Biology* 58:468–477.
- LYON, M. W. 1906. Mammals of Banka, Mendanau, and Billiton Islands, between Sumatra and Borneo. *Proceedings of the United States National Museum* 31:575–612.
- LYON, M. W. 1911. Mammals collected by Dr. W. L. Abbott on Borneo and some of the small adjacent islands. *Proceedings of the United States National Museum* 40:53–146.
- LYON, M. W. 1913. Treeshrews: an account of the mammalian family Tupaiidae. *Proceedings of the United States National Museum* 45:1–188.
- MARTIN, R. D. 1968. Reproduction and ontogeny in tree shrews (*Tupaia belangeri*), with reference to their general behavior and taxonomic relationships. *Zeitschrift für Tierpsychologie* 25:409–532.
- MEIJAARD, E., AND J. MACKINNON. 2008. *Tupaia chrysogaster*. In: IUCN 2011. IUCN Red list of threatened species. Version 2011.1. www.iucnredlist.org. Accessed 20 August 2011.
- MEREDITH, R. W., ET AL. 2011. Impacts of the Cretaceous terrestrial revolution and KPg extinction on mammal diversification. *Science* 334:521–524.
- MILLER, G. S. 1903. Seventy new Malayan mammals. *Smithsonian Miscellaneous Collections* 45:1–73.
- MURPHY, W. J., ET AL. 2001. Resolution of the early placental mammal radiation using Bayesian phylogenetics. *Science* 294:2348–2351.
- MYERS, N., R. A. MITTERMEIER, C. G. MITTERMEIER, G. A. B. DA FONSECA, AND J. KENT. 2000. Biodiversity hotspots for conservation priorities. *Nature* 403:853–858.
- NAPIER, J. R., AND P. H. NAPIER. 1967. *A handbook of living primates*. Academic Press, New York.
- OLSON, L. E., S. M. GOODMAN, AND A. D. YODER. 2004a. Illumination of cryptic species boundaries in long-tailed shrew tenrecs (Mammalia: Tenrecidae; *Microgale*), with new insights into geographic variation and distributional constraints. *Biological Journal of the Linnean Society* 83:1–22.
- OLSON, L. E., E. J. SARGIS, AND R. D. MARTIN. 2004b. Phylogenetic relationships among treeshrews (Scandentia): a review and critique of the morphological evidence. *Journal of Mammalian Evolution* 11:49–71.
- OLSON, L. E., E. J. SARGIS, AND R. D. MARTIN. 2005. Intraordinal phylogenetics of treeshrews (Mammalia: Scandentia) based on evidence from the mitochondrial 12S rRNA gene. *Molecular Phylogenetics and Evolution* 35:656–673.
- OLSON, L. E., AND A. D. YODER. 2002. Using secondary structure to identify ribosomal numts: cautionary examples from the human genome. *Molecular Biology and Evolution* 19:93–100.
- OWEN, R. 1866. *On the anatomy of the vertebrates. II. Birds and mammals*. Longmans, Green, London, United Kingdom.
- RAFFLES, T. S. 1821. Descriptive catalogue of a zoological collection, made on account of the honourable East India Company, in the island of Sumatra and its vicinity, under the direction of Sir Thomas Stamford Raffles, Lieutenant-Governor of Fort Marlborough; with additional notices illustrative of the natural history of those countries. *Transactions of the Linnean Society of London* 13:239–274.
- ROBERTS, T. E., H. C. LANIER, E. J. SARGIS, AND L. E. OLSON. 2011. Molecular phylogeny of treeshrews (Mammalia: Scandentia) and the timescale of diversification in Southeast Asia. *Molecular Phylogenetics and Evolution* 60:358–372.
- ROBERTS, T. E., E. J. SARGIS, AND L. E. OLSON. 2009. Networks, trees, and treeshrews: assessing support and identifying conflict with multiple loci and a problematic root. *Systematic Biology* 58:257–270.

- ROBINSON, H. C. AND C. B. KLOSS. 1914. On new mammals, mainly from Bandon and the adjacent islands, east coast of the Malay peninsula. *Annals and Magazine of Natural History* 13:223–234.
- SARGIS, E. J. 2001. A preliminary qualitative analysis of the axial skeleton of tupaiids (Mammalia, Scandentia): functional morphology and phylogenetic implications. *Journal of Zoology (London)* 253:473–483.
- SARGIS, E. J. 2002a. Functional morphology of the forelimb of tupaiids (Mammalia, Scandentia) and its phylogenetic implications. *Journal of Morphology* 253:10–42.
- SARGIS, E. J. 2002b. Functional morphology of the hindlimb of tupaiids (Mammalia, Scandentia) and its phylogenetic implications. *Journal of Morphology* 254:149–185.
- SCHLICK-STEINER, B. C., B. SEIFERT, C. STAUFFER, E. CHRISTIAN, R. H. CROZIER, AND F. M. STEINER. 2007. Without morphology, cryptic species stay in taxonomic crypsis following discovery. *Trends in Ecology & Evolution* 22:391–392.
- SHAMEL, H. H. 1930. Mammals collected on the island of Koh Tau off the east coast of the Malay Peninsula. *Journal of Mammalogy* 11:71–74.
- SODHI, N. S., L. P. KOH, B. W. BROOK, AND P. K. L. NG. 2004. Southeast Asian biodiversity: an impending disaster. *Trends in Ecology & Evolution* 19:654–660.
- STAFFORD, B. J., AND R. W. THORINGTON, JR. 1998. Carpal development and morphology in archontan mammals. *Journal of Morphology* 235:135–155.
- STEELE, D. G. 1983. Within-group variation in coat-color characteristics of the common tree shrew, *Tupaia glis* Diard, 1820. *International Journal of Primatology* 4:185–200.
- THOMAS, O. 1893. On some new Bornean Mammalia. *Annals and Magazine of Natural History* 11:341–347.
- THOMAS, O. 1895. On some mammals collected by Dr. E. Modigliani in Sipora, Mentawai Islands. *Annali. Museo Civico de Storia Naturale Genoa ser. 2* 14:661–672.
- THOMAS, O. 1917. Scientific results from the mammal survey no. XVI. (A) The tupaia of south Tenasserim. *Journal of the Bombay Natural History Society* 25:199–201.
- VAUGHAN, T. A. 1970. The skeletal system. Pp. 97–138 in *Biology of bats* (W. A. Wimsatt, ed.). Academic Press, New York. Vol. 1.
- WAGNER, J. A. 1841. Schreber's Saugthiere, Supplementband, 2. Abtheilung 1841:37–44, 553.
- WEISBECKER, V., AND S. SCHMID. 2007. Autopodial skeletal diversity in hystricognath rodents: functional and phylogenetic aspects. *Mammalian Biology* 72:27–44, 553.
- WILSON, D. E. 1993. Order Scandentia. Pp. 131–133 in *Mammal species of the world: a taxonomic and geographic reference* (D. E. Wilson and D. M. Reeder, eds.). 2nd ed. Smithsonian Institution Press, Washington, D.C.
- WOODMAN, N. 2010. Two new species of shrews (Soricidae) from the western highlands of Guatemala. *Journal of Mammalogy* 91:566–579.
- WOODMAN, N. 2011. Patterns of morphological variation amongst semifossorial shrews in the highlands of Guatemala, with the description of a new species (Mammalia, Soricomorpha, Soricidae). *Zoological Journal of the Linnean Society* 163:1267–1288.
- WOODMAN, N., AND J. J. P. MORGAN. 2005. Skeletal morphology of the forefoot in shrews (Mammalia: Soricidae) of the genus *Cryptotis*, as revealed by digital X-rays. *Journal of Morphology* 266:60–73.
- WOODMAN, N., AND R. B. STEPHENS. 2010. At the foot of the shrew: manus morphology distinguishes closely-related *Cryptotis goodwini* and *Cryptotis griseiventris* (Mammalia: Soricidae) in Central America. *Biological Journal of the Linnean Society* 99:118–134.

Submitted 30 September 2011. Accepted 24 June 2012.

Associate Editor was Brian S. Arbogast.

APPENDIX I

Taxa and specimens examined.

All specimens in this study are from the Division of Mammals, United States National Museum of Natural History (USNM), Smithsonian Institution, Washington, D.C., and catalog numbers pertain to that institution. Taxa are separated into the final 8 taxa we recognized in this study. Subspecies names are meant as a guide to the populations included in each of the species we recognize herein. In addition to providing historical perspective to specimens (e.g., Lyon 1913), these names provide a sense of the geographic diversity still present in the taxa we studied.

Tupaia belangeri ($n = 74$).—Described as *Cladobates belangeri* Wagner, 1841, from Burma. This taxon was considered a species by Lyon (1913), but has often been included in *T. glis* over the last century (e.g., Honacki et al. 1982). More recently, it has been recognized as a separate species (Corbet and Hill 1992; Dene et al. 1978; Helgen 2005; Olson et al. 2005; Roberts et al. 2009, 2011; Wilson 1993).

Tupaia belangeri cambodiana ($n = 15$).—THAILAND: Chanthaburi: Khao Sabab (258926, 258929, 535150, 535151); Hup Bon (256885); Nong Khon (241065, 241453). Nakhon Ratchasima: Lat Bua Khao (221574); Lam Khlong Lang (241452); Ban Pak Chong (251693); Lat Bua Khao (254757). Trat: Ok Yam (201430); Klong Yai (201431); Khao Saming (256884, 535152).

Tupaia belangeri cochinchinensis ($n = 1$).—VIETNAM: Dong Nai; Bein Hoa (258008).

Tupaia belangeri dissimilis ($n = 16$).—VIETNAM: Ba Ria-Vung Tau; Con Son Island (357003–357006, 357188, 357189, 357191–357193, 357247, 357249–357254).

Tupaia belangeri kohtauensis ($n = 9$).—THAILAND: Surat Thani: Koh Tau (252241–252247, 253444, 253445).

Tupaia belangeri laotum ($n = 3$).—THAILAND: Tak: Me Taque (253566); Nan: Ban Nam Kien (255758); Lamphun: Khun Tan Mountains (257817).

Tupaia belangeri lepcha ($n = 2$).—INDIA: Bengal: Sangsir (260739). NEPAL: Chatra (290063).

Tupaia belangeri olivacea ($n = 15$).—THAILAND: Samut Sakhon: Tachin (221561). Phra Nakhon Si Ayutthaya: Montaburi (240046); Bangkok (241058, 241059, 241062, 241063, 257819). Kanchanaburi: Muang Kan Buri (253448). Chiang Mai: Chieng Dao (257816). Nakhon Sawan: Pak Nam Pho (296891–296895, 296900).

Tupaia belangeri siamensis ($n = 3$).—THAILAND: Prachuap Khiri Khan: Koh Lak (221576, 221577, 221578).

Tupaia belangeri siccata ($n = 1$).—INDIA: Manipur: Imphal (279178).

Tupaia belangeri sinus ($n = 2$).—THAILAND: Trat: Koh Chang (201435, 201436).

Tupaia belangeri tenaster ($n = 1$).—MYANMAR: Tanintharyi (Tenasserim): Mergui Archipelago, Victoria Point (124003).

Tupaia belangeri tonquinia ($n = 1$).—LAOS: Salavan: Thateng (260738).

Tupaia belangeri versurae ($n = 1$).—INDIA: Assam: Ledo (279321).
Tupaia belangeri ssp. ($n = 4$).—MYANMAR: Bago: Dawe, Bago Yoma Mts. (583794, 583796). Mandalay: Pyin-Oo-Lwin (Maymyo) (584375, 584376).

Tupaia chrysogaster ($n = 12$).—Described as *Tupaia chrysogaster* Miller, 1903, from the Mentawai Islands off the west coast of Sumatra (Fig. 9). Considered a species by Lyon (1913), it was synonymized with *T. glis* by Chasen (1940), and it retained this status (e.g., Corbet and Hill 1992) until the species was resurrected by Wilson (1993:132), who stated that it “[m]ay prove to be only a subspecies of *glis*.” Now recognized as a distinct species (Helgen 2005), the separation of *T. chrysogaster* from *T. glis* is additionally supported by molecular data (Roberts et al. 2011).

INDONESIA: Pagai Utara Island (type locality) (121571, 121573, 121575); Pagai Selatan Island (121577, 121579); Sipora Island (252330–252333, 252335, 252337, 252338).

Tupaia glis ($n = 35$).—Described as *Sorex glis* Diard, 1820, from Penang Island, along the west coast of the Malay Peninsula, this was the 1st species of treeshrew described. Lyon (1913) included 6 subspecies in this taxon.

Tupaia glis anambae ($n = 2$).—INDONESIA: Kepulauan Riau: Riau Archipelago; Djemadja Island (101741, 101742).

Tupaia glis batamana ($n = 1$).—INDONESIA: Kepulauan Riau: Riau Archipelago; Batam Island (142152).

Tupaia glis castanea ($n = 1$).—INDONESIA: Kepulauan Riau: Riau Archipelago; Bintang Island (115607).

Tupaia glis ferruginea ($n = 1$).—SINGAPORE (124317). [Referred to *T. g. ferruginea* by Lyon (1913).]

Tupaia glis lacernata ($n = 13$).—MALAYSIA: Kedah: Pulo Langkawi (type locality) (104353, 123901).

THAILAND: Satun: Pulo Terutau (123981, 123982, 123985, 123987). Trang: Trang (83254, 83257, 83477); Khao Sai Dao (258927); Khao Chong (258928); Telibon Island (83256). Nakhon Si Thammarat: Seechol (255754).

Tupaia glis phaoura ($n = 2$).—INDONESIA: Kepulauan Riau: Lingga Archipelago, Singkep Island (113147, 113149).

Tupaia glis raviana ($n = 1$).—THAILAND: Satun: Butang Islands, Pulo Adang (104354).

Tupaia glis siberu ($n = 2$).—INDONESIA: Siberut Island (252328, 252329).

Tupaia glis sordida ($n = 11$).—MALAYSIA: Pahang: Pekan District, Tioman Island (101746, 104973–104976, 487932–487934, 487936–487938).

Tupaia glis ultima ($n = 1$).—THAILAND: Surat Thani: Koh Phangan Island (256882).

Tupaia discolor ($n = 6$).—Described as *Tupaia discolor* Lyon, 1906, from Bangka Island off the east coast of Sumatra (Fig. 9). Not surprisingly, this taxon was recognized as a distinct species by Lyon (1913) but was later synonymized with *T. glis* by Chasen (1940), and it has generally been considered a synonym of that species (Corbet and Hill 1992; Helgen 2005; Honacki et al. 1982; Wilson 1993). Unlike *T. glis*, however, *T. discolor* possesses 6 mammae (Table 1). We include all specimens from Bangka Island in this species.

INDONESIA: Kepulauan Bangka Belitung: Pulau Banka (124701, 124702, 124704, 124705, 124706, 124904).

Tupaia ferruginea ($n = 13$).—Described as *Tupaia ferruginea* Raffles, 1821, from Bencoolen, Sumatra. Considered a subspecies of *T. glis* by Lyon (1913:42), who noted “I have been able to find no essential differences between specimens from the Malay Peninsula and the island of Sumatra.” This taxon generally remains in synonymy with *T. glis* (Chasen 1940; Corbet and Hill 1992; Helgen 2005; Honacki et al. 1982; Wilson 1993). For this study, we include all populations of *T. glis* from Sumatra in this species (Fig. 9).

Tupaia glis ferruginea ($n = 5$).—INDONESIA: Sumatra: Tarussan Bay (141074); Loh Sidoh Bay (114152, 114153); Aru Bay (143329, 143333).

Tupaia glis jacki ($n = 2$).—INDONESIA: Sumatra: Tapanuli Bay (114548, 114549).

Tupaia glis phoeniura ($n = 4$).—INDONESIA: Sumatra: Perlak, Atjeh (257593, 257594, 257595, 257596).

Tupaia glis siaca ($n = 2$).—INDONESIA: Sumatra: Little Siak River (144204, 144209).

Tupaia “glis” hypochrysa ($n = 1$).—Described as a subspecies, *Tupaia ferruginea hypochrysa* Thomas, 1895, from Java (Fig. 9). This taxon was elevated to species by Lyon (1913:71), who noted “*Tupaia hypochrysa* is probably the Javan representative of *T. glis ferruginea*, yet it is a very distinct species.” Lyon (1913) included this taxon with *T. chrysogaster* in his “Hypochrysa Group.” The taxon was subsequently synonymized with *T. glis* by Chasen (1940), and this remains its current status (Helgen 2005; Honacki et al. 1982; Wilson 1993). Our sample consists of only a single specimen, but this specimen is sufficiently distinct to indicate that this taxon may warrant recognition as a separate species.

INDONESIA: Java: Gunung Salak (154599).

Tupaia longipes ($n = 3$).—Described as *Tupaia ferruginea longipes* Thomas, 1893, from northern (Malaysian) Borneo, *T. longipes* was recognized as a separate species by Lyon (1911). It was subsequently synonymized with *T. glis* by Chasen (1940), and it was long considered as a member of that species (Corbet and Hill 1992; Honacki et al. 1982), despite having 6 mammae (Table 1). *T. longipes* has since been recognized as a distinct species, but generally with *T. salatana* included as a subspecies (Dene et al. 1978; Helgen 2005; Wilson 1993). Here, we restrict this species to northern Borneo (Fig. 9).

MALAYSIA: Sabah: Borneo, no specific locality (396673); Kampong Morok (488034); Poring (488045).

Tupaia salatana ($n = 4$).—Described as *Tupaia longipes salatana* Lyon, 1913, from southern (Indonesian) Borneo, this taxon was synonymized with *T. glis* by Chasen (1940) and long considered as such (Corbet and Hill 1992; Honacki et al. 1982). It has only recently been recognized once again as a subspecies of *T. longipes* by Helgen (2005). We refer southern populations of *T. longipes* on Borneo to *T. salatana* (Fig. 9).

INDONESIA: Borneo: Sungai Pelawan (198040, 198041, 198043); Sungai Djambajan (199162).